Doctoral Thesis
博士論文

Dependable learning scheme of model for predicting drug dosage effect in a human body using recurrent neural networks

人体の投薬効果予測のモデルのためのリカレントニューラルネットワークを用いた高信頼学習

March 25th, 2021
2021 年 3 月 25 日

18QC502
Yoshitomo SAKUMA
佐久間 義友

Supervisor: Professor Ryuji KOHNO
指導教官： 河野隆二 教授

Department of Mathematics, Physics, Electrical Engineering and Computer Science, Graduate School of Engineering Science, Yokohama National University, Kohno Laboratory
横浜国立大学大学院 理工学府
数物・電子情報系理工学専攻 河野研究室

Table of Contents

List of Figures

List of Tables

Acknowledgements

First of all, I ' d like to thank my supervisors, Prof. Ryuji Kohno, Ass. Prof. Chika Sugimoto, Dr. Takumi Kobayashi, Dr. Kento Takabayashi, and Dr. Minsoo Kim for these guidance and encouragement in helping me accomplish this thesis. Without their sincere and whole hearten supervision, this work would not have been possible. Apart from the academic side, their continuous encouragement and moral support made my life easy. To all the members of Kohno laboratory, I ' d like to express my appreciation for the positive atmosphere and all the friendly advice given to me. I ' d like to thank my friends and all those who have helped me and contributed somehow to the successful completion of this thesis. Finally, I would like to express my sincere gratitude to my family for giving me the opportunity to pursue my doctorate degree.

Abstract

In recent years, with the development of technologies such as the Internet of Things (IoT) and cyber-physical systems (CPS), research that applies them to various fields has attracted attention. In particular, with the aging society and the shortage of medical staff, the demand for research on medical ICT that applies information and communication technology to medical care is increasing.

Among them, the anesthesia control technology during surgery is that can reduce the burden on anesthesiologists, which is lacking in the medical field, and is expected to contribute to the efficiency and reliability of medical care. In order to control proper anesthesia, it is necessary to meet various restrictions and requirements based on medical knowledge and laws. The medical guidelines provide guidelines for dosages that take patient safety into consideration, which is one of the restrictions in anesthesia control. In addition, while satisfying these restrictions, the BIS (Bispectral index) value used to evaluate the sedative effect of anesthesia during surgery and the vital vitality for evaluating the analgesic(pain reduction) effect such as pulse wave and heart rate (HR) should be within an appropriate range. It is also required that the time from the start of surgery until various vitals fall within the appropriate range (anesthesia induction time) and the time until the BIS value after the end of surgery returns to the value at which the patient awakens are as short as possible.

On the other hand, the population of diabetic patients is increasing worldwide, and maintaining good health is becoming a social issue. In particular, insulin therapy for diabetics is based on blood sugar levels in daily life, including sleep. The dose must be calculated administered by the patient, which imposes a heavy psychological burden for them. In addition, the number of patients with congenital type 1 diabetes called childhood diabetes is increasing. However, if the patient is a child, there is also an increased risk of accidents such as forgetting to take improper doses or administering them.

For both problems of anesthesia and blood glucose control using insulin for diabetic patients, methods for controlling the desired value have been studied.

In those studies vital changes due to medication are predicted using a model. However, there is a problem that existing numerical models do not completely take into account individual differences of patients and time-varying effects of drugs that change from moment to moment.

Based on these problems, this thesis proposes a predictive control system for patient vitals based on this study using a recurrent neural network (RNN). In the proposed system, RNNs are used to model patient efficacy as a non-linear time-varying system.

In the proposed system, in this study, in improving the identification (learning) accuracy of the prediction model by RNN, two main problems were raised and proposals were made for each.

One is the stochastic gradient descent method (SGD), which is generally used for learning RNNs. In SGD, there is a problem that the estimation accuracy of the model changes depending on the value learning rate. In this study, we analysed theoretically the relationship between the learning rate and the learning stability, and proposed a method of adaptively updating the learning rate under the condition that the stability of the RNN can be guaranteed.

Secondly, if the vital data used for model training contains artifacts due to measurement errors or contamination with other vitals such as ECG, there is a problem that the identification accuracy may decrease due to the artifacts. In this study, a method to detect artifacts from the context of vital data is proposed. In particular, this thesis proposes a method specialized in detecting instantaneous artifacts such as R waves of ECG, and erroneous due to the detection threshold. Also, it is considered that the detected / undetected trade-off and its effect on vital estimation using RNN.

あらまし

近年，Internet of Things (IoT) や Cyber Physical System (CPS) などの技術の発展に伴い，これらを様々な分野に応用した研究への注目が集まっている．特に，高齢化社会や医療従事者の不足といった問題に伴い，情報通信技術を医療へ応用した医療 ICT の研究の需要は高くなっている．

その中でも，手術中における麻酔の制御技術は医療現場において不足している麻酔医の負担を軽減できる技術であることから，医療の効率化や高信頼化への貢献が期待されている．高信頼な麻酔の制御を行うためには，医学的な知見や法律に基づいた様々な制約や要求を満たす必要がある．法律に基づいたガイドラインや文章には，患者の安全を考慮した投与量の目安が記載されており，これが麻酔制御における制約として挙げられる．また，その制約を満たしつつ手術中の麻酔による鎮静作用評価に用いられる BIS　(Bispectral index) 値や，脈波・心拍 (HR: Heart rate) などから得られる鎮痛作用評価に用いられるバイタルを適切な範囲に収めること，手術開始してから各種バイタルが適切な範囲に収まるまでの時間（麻酔導入時間）および手術終了してから患者が覚醒するまでにかかる時間がなるべく短くなることが要求される．

一方で，糖尿病患者の人口も世界的に増加傾向にあり，彼らの健康維持も一つの社会問題となっている．特に, 糖尿病患者のインスリン療法は日常生活で睡眠時も含めた血糖値に基づいて投与量を計算して自己投与しなければならず，患者に対する精神的負担も大きい．そして小児糖尿病と呼ばれる先天的な 1 型糖尿病患者も増加しているが，患者が小児の場合は投与を忘れることや不適切な量を投与してしまうなどの事故のリスクも増加すると考えられる．

これらの，手術中麻酔および糖尿病患者へのインスリンを用いた血糖値制御という問題に対して，医師および患者の負担軽減および安全保障のために投薬によるバイタル変化を，数値モデルを用いて予測しバイタル値を所望の値に制御するための方式が研究されているが，既存の数値モデルは患者の個人差や時々刻々と変化する薬の効き方の時変性まで考慮されてないという問題がある．これらの問題に基づいて，本研究ではリカレントニューラルネットワーク（RNN）を使用した予測に基づく患者のバイタルの予測制御システムを提案した．提案されたシステムでは，患者の薬効を非線形時変システムと仮定し RNN によってモデル化し

ている．

提案システムにおいて本研究では，RNN による予測モデルの同定（学習）精度を向上させるにあたり主に二つの問題を提起しそれぞれに対して提案を行った．一つ目の問題として，RNN の学習に一般的に用いられる確率的勾配降下法（SGD）についてであるが，SGD では設定した学習率によりモデルの推定精度が変化してしまうという問題がある．その問題に対して本研究では，学習率と学習安定性の関係を理論的に解析し，RNN の安定性が保証できる条件を満たすように学習率を適応的に更新する方法を提案した．また，モデルの学習に用いるバイタルデータに測定ミスや ECG などのほかのバイタルの混入によるアーティファクトが含まれる場合，アーティファクトによって同定精度が低下する恐れがあるという問題がある．その問題に対して本研究では，アーティファクトをバイタルデータの前後関係から検出する手法を提案した．特に，ECG の R 波などの瞬時的なアーティファクトの検出に特化した手法を本研究では提案し，検出閾値による誤検出・未検出のトレードオフおよびそれが RNN を用いたバイタル推定に及ぼす影響を考察した．

Chapter 1

Introduction

In recent years, services that can make people life convenient, such as cyber-physical systems (CPS), have been attracting attention. Along with this, the application of machine learning (ML) and data science to the medical field is being studied to support the medical field, which is in a difficult situation due to the aging population and the shortage of medical staffs [4, 5, 6].

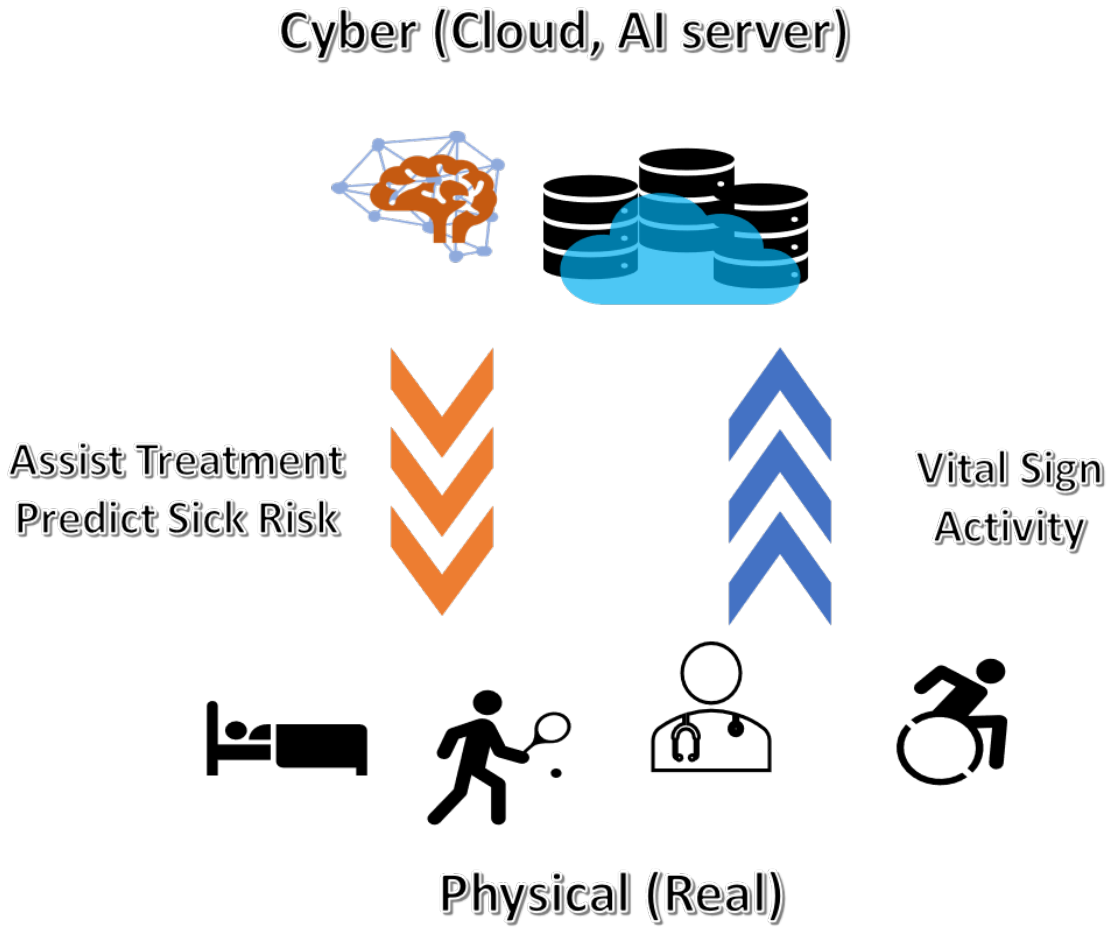

Figure 1.1 Cyber Physical System (CPS) for medical application

The shortage of medical staff,(e.g., anesthesiologists) presents major problem [7, 8]. The shortage of anesthesiologists may lead to poor management of the patient's anesthesia and an increased risk of postoperative sequelae. To ameliorate this problem and to ensure the safety of surgical operations, dosage control systems for total intravenous anesthesia (TIVA) have been proposed [9, 10].

While, as another problem, The population of diabetics is also increasing around the world [11], and maintaining their health has become a social problem. In particular, insulin therapy for diabetic patients imposes a heavy mental burden on the patients because the patients themselves adjust the dose based on the blood glucose level even during sleep in daily life. In addition, the number of patients with congenital type 1 diabetes called childhood diabetes is increasing, but in the case of children, the risk of accidents such as forgetting to administer or administering an inappropriate amount is thought to increase. Based on these issues, glycemic control systems using glycemic sensors and insulin pumps have been studied for the treatment of diabetic patients [11] [12].

To improve performances of those dosage control system, control method using model predictive control (MPC) were proposed [13, 14, 15, 16, 17, 18]. The MPC method is effective to control complex conditions such as maintaining patient health, assuming the model is accurate. As the model of the drug effect in human body, the parametric model was built with the assumption that drug absorption in the human body is limited to four fluid compartments. Moreover, scientific researchers have proposed the estimation scheme of time variation of vital value using a parametric model [19, 20] and extended Kalman filter (EKF) [21, 22].

However, although the relationship between drug concentration in the human body and drug effect assumed to be estimated by nonlinear equation [20], the full picture of the action mechanism of drugs is much more complicated. There are more hidden factors like degradation of the liver function through alcoholic liver disease [23] or stimulation to the patients by the treatment during surgery [17, 18].

Considering those problems, this paper proposes an estimation system of time transition of vital value using recurrent neural network (RNN). Since the vital changes due to drug administration can be assumed to be a nonlinear time-varying system, in this study, the model constructed by RNN was applied in order to predict the dosing response.

Figure 1.2 shows the conceptual diagram of our proposed system.

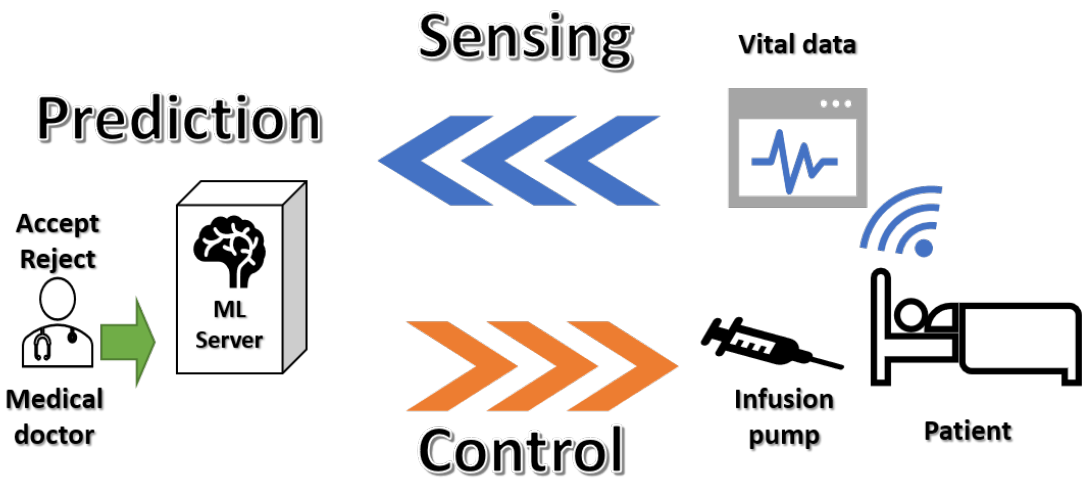

Figure 1.2 The conceptual diagram of the proposal

The flow of the processing is as follows:

Step1. The vital monitors measures the current vital value of the patient.

Step2. The vital monitors sends the current vital value to the ML server.

Step3. The ML server updates the RNN model using the current vital values with following learning algorithm.

Step4. The ML server calculates the optimum dosage by the prediction using RNN model.

Step5. If the medical doctors accepted the optimized dosage, The ML server sends the control command (the optimized dosage) to the infusion pump. Otherwise, the medical doctors decides the dosage.

Step6. The dosage controller controls the infusion pump based on the received command.

Step7. Back to the Step 1 and repeat the Step 1-6 until the infusion is finished.

In general, stochastic gradient descent (SGD) is used to learn neural networks. However, the stability of the scheme learned by SGD dependent on the learning rate to update the network parameters. In previous research on similar issues, although other scientific researchers proposed an estimation scheme of time

transition of drug effects using neural networks [24, 25, 26], the stability of those schemes were not discussed. Hence, this paper proposes learning the prediction model using the RNN to predict the anesthetic effect considering the network stability.

In addition, vital data may contain artifacts due to measurement errors and contamination by other vital signals (ECG, EMG, etc.). Learning RNNs with data that contains artifacts and predicting significant changes causes the problem of poor estimation performance. Based on this, in this study, it is proposed that an artifact detection and removal method using difference value information, assuming that the sample values of the vital data before and after are close to each other when the artifact is not included.

The main contribution and novelty of the manuscript are as follows

1. The stability of the RNN is analyzed based on Lyapunov analysis [27, 28]. From the analysis, the condition of the stability and optimum learning rate for each parameter in the RNN model are derived. Furthermore, the manuscript proposes the scheme that learning rate updates adaptability and make identification speed faster within a condition of stability.

2. To prevent the prediction performance from deteriorating due to the artifacts of each vital, this thesis proposes an artifact detection method based on the difference before and after the vital data. Then, the trade-off between false positive and false negative of the artifact detection performance based on the threshold value of the proposed detection method was theoretically analyzed.

3. Novel performance evaluations considering various patient are conducted. Especially, the proposed method was compared with the existing learning methods SGD, RMSprop, and Adam. From the evaluation, the efficiency of our proposed scheme is confirmed and discussed. Also, it is confirmed and discussed that the case where the performance of proposal became lower compared with existing method.

This paper is organized as follows. In Chap.2, related description and problems about ML for application of drug administration. In Chap. 3, the whole system model of the proposed scheme is explained. In Chap. 4, modeling and estimation scheme of drug effect using RNN is explained. In Chap. 5, the dependable learning algorithm based on theoretical analysis of the learning

stability is performed and the optimum learning rate is discussed. In Chap. 6, the pre-processing method of the vital data for the artifact detection and cancellation is explained. in Chap. 7, conclusions our work and discussion of the future research are described.Figure 1.3 shows the relation of these chapters in the paper.

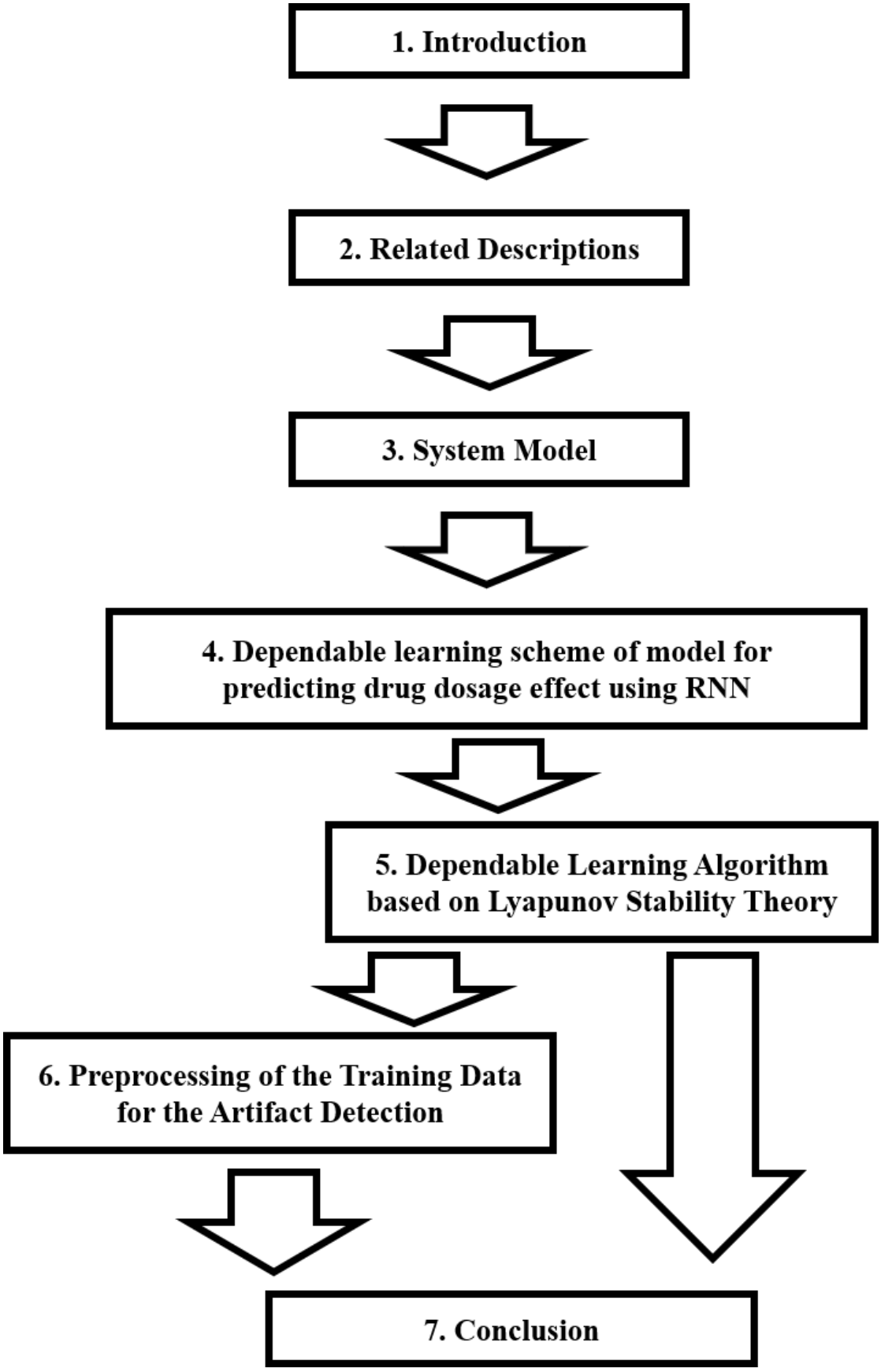

Figure 1.3 Flowchart of the thesis

Chapter 2

Related Description

2.1 Existing study to predict drug effect using Neural Networks

2.1.1 Overview of the related study

In the section, the related description about vital estimation using Neural Networks. Several studies have proposed methods for predicting vital changes due to medication. In the paper[24, 25], prediction scheme of blood glucose level using Neural Networks is proposed. Moreover, in the paper[26] prediction scheme the behavior of vital that indicates hypnotic and analgesic effect using Neural Network.

However, there is a problem that these studies do not theoretically decide the hyper-parameters of neural networks. In particular, for existing learning methods (e.g. SGD ,RMSprop, Adam), The learning speed accuracy changes depending on the parameter design.In addition, it is considered that the optimum values of the parameters that determine the learning speed to differ depending on the handled data and the patient to be estimated. Therefore, considering that it is for medical use, it can be said that it is necessary to theoretically support the parameters used for learning in order to guarantee the accuracy of prediction.

In addition, vital data sometimes contains electrical signals derived from other vitals called artifacts. It can be said that the prediction accuracy will decrease if learning is performed using data that includes artifacts. However, there is a problem that the method for detecting artifacts has not been examined in existing studies[24, 25, 26].

2.1.2 Existing learning algorithm of neural networks

Here, existing learning method to update weights in neural networks.

Stochastic Gradient Decent(SGD)[29, 30]

Stochastic Gradient Descent (SGD)[29, 30] is one of the gradient methods used for learning neural networks. This method is different from the gradient descent method in that training is performed using only one sample of the training data. Therefore, it can be used for online learning of neural network models.The neural network weight update formula by SGD is as follows:

$$w[t+1] = w[t] - \mu \frac{\partial E[t]}{\partial w[t]}, \tag{2–1}$$

where, $w[t]$ is the weighting coefficient in the neural network, $E[t]$ is the evaluation function of learning, and μ is the learning rate that determines the learning speed. As shown in the e.q (2–1), if the learning rate is too small, the weight of neural networks will not converge to the optimum solution. Another problem is that if the learning rate is too large, learning becomes unstable and the optimum solution cannot be reached. Therefore, it is important to properly determine this learning rate in order to guarantee the learning performance of neural networks.

RMSprop[31]

RMSprop[31] is one of the improved methods of SGD mentioned above. Specifically, in RMSprop, the learning rate can be adaptively changed in consideration of the gradient in the past time, thereby preventing the learning from becoming unstable due to a sudden change in the gradient. The neural network weight update formula by RMSprop is as follows:

$$\begin{aligned} v[t+1] &= \beta v[t] + (1-\beta)(\frac{\partial E[t]}{\partial w[t]})^2 \\ w[t+1] &= w[t] - \frac{\mu}{\sqrt{v[t+1]+\epsilon}} \frac{\partial E[t]}{\partial w[t]}, \end{aligned} \tag{2–2}$$

where, $v[t]$ is moving average of the the square of the gradient of each weights, β is the parameter that determines the rate of previous moving average, and μ is the parameter that determines impact of the current gradient on learning, and ϵ is the parameter to prevent division by zero. As shown in the e.q (2–2), since the learning rate adaptively changes according to the moving average of

the gradient magnitude so far, divergence due to abrupt gradient changes is less likely to occur compared to SGD. However, RMSprop also has the problem that the learning result depends on the parameter setting.

Adam[32]

Adam[32] is a learning method that is a further improvement of the above-mentioned RMSprop. Specifically, by using not only the absolute value of the gradient but also the moving average of the gradient itself, it is possible to prevent learning from becoming unstable at the point where the positive and negative of the gradient changes. The neural network weight update formula by Adam is as follows:

$$
\begin{aligned}
v[t+1] &= \beta_1 v[t] + (1-\beta_1)(\frac{\partial E[t]}{\partial w[t]}) \\
s[t+1] &= \beta_s v[t] + (1-\beta_s)(\frac{\partial E[t]}{\partial w[t]})^2 \\
w[t+1] &= w[t] - \frac{\mu v[t+1]}{\sqrt{s[t+1]+\epsilon}},
\end{aligned} \tag{2–3}
$$

where, $v[t]$ is moving average of the gradient of each weights,$v[t]$ is moving average of the squared gradient in each weights, β_1 and β_2 are the parameters that determines the rate of previous moving average, and μ is the parameter that determines moving average of the gradient of each weights $v[t]$, and ϵ is the parameter to prevent division by zero. Adam is an improved version of RMSprop, but the problem remains that performance depends on parameter settings.Although Recommended parameters are also described in the paper[32], depending on the problem, another better parameter need to be searched.

2.2 Problem in Total intravenous anesthesia case

2.2.1 Overview of demands in total intravenous anesthesia

The shortage of anesthesiologists may lead to poor management of the patient's anesthesia and an increased risk of postoperative sequelae. To ameliorate this problem and to ensure the safety of surgical operations, dosage control systems for total intravenous anesthesia (TIVA) have been proposed [9, 10]. Generally, the administration of anesthesia during surgery for sedation, analgesia, and muscle relaxation of patients has to guarantee patient's satisfy after the

operation [33]. For example, the constrained dosage propofol [34] for sedation and the physiological information indicating anesthetic depth has to be taken into consideration. Thus the bispectral index (BIS) [1] is often used as an index of anesthetic depth. Table 2.1 shows the relationship between the BIS value and the patients' condition. Hence. it shows that the desired BIS value during surgery ranges from 40 to 60.

Table 2.1 Bispectral Index [1]

Condition of the patients	Value of BIS
Awaken	From 90 to 100
Light Hypnosis	From 60 to 90
Desired range	From 40 to 60
Deep Hypnosis	From 0 to 40

2.2.2 Problem in prediction anesthetic effect using recurrent neural network

Here, the problems in predicting the effect of anesthetics using a recurrent neural network are described. One problem is that it is necessary to study the interaction of multiple drugs when predicting the anesthetic effect during surgery. Specifically, since sedatives and analgesics mutually affect vital signs such as BIS value, a learning model that takes this into consideration is required. Another problem is that various vitals are assumed to measure during surgery. Hence, the artifacts from each vital have to be considered during learning of RNN model. In particular, it has been reported that EMG and ECG-derived artifacts are mixed in the BIS value[35, 36]. Therefore, it is necessary to perform pre-processing to remove the artifacts before using the BIS value as training data.

Chapter 3

System Model

In this section, the process of our proposed system in details is described.

3.1 Overview of the proposed system

3.1.1 Novelty of the proposed system

First, the novelty of this study is described in this section. The novelty of this study is that in addition to the conventional prediction of drug effects by neural networks, this thesis proposes a learning method to make the estimation performance highly reliable. In order to perform model predictive control of drug dose, it is necessary to guarantee the estimated performance by the model. Based on this, the following two proposals were made in this study.

1. The stability of the RNN is analyzed based on Lyapunov analysis [27, 28]. From the analysis, the condition of the stability and optimum learning rate for each parameter in the RNN model are derived. Furthermore, the manuscript proposes the scheme that learning rate updates adaptability and make identification speed faster within a condition of stability.

2. To prevent the prediction performance from deteriorating due to the artifacts of each vital, this thesis proposes an artifact detection method based on the difference before and after the vital data. Then, the trade-off between false positive and false negative of the artifact detection performance based on the threshold value of the proposed detection method was theoretically analyzed.

3.1.2 Applicable class of the proposed system

The classes (problems) assumed to be applied in this study are described in this section. First, the problem envisioned in this study is the system identification problem of significant changes to human medication using RNN. Specifically, it is assumed that change of the vital (output) by administration (input) is predicted using RNN. In this system, RNN is used to model the medication effects of patients. Also, it is assumed that learning of RNN is performed by vitals sensed from the patient.

3.2 Structure of the proposed system

Figure 3.1 shows the diagram of our proposed system.

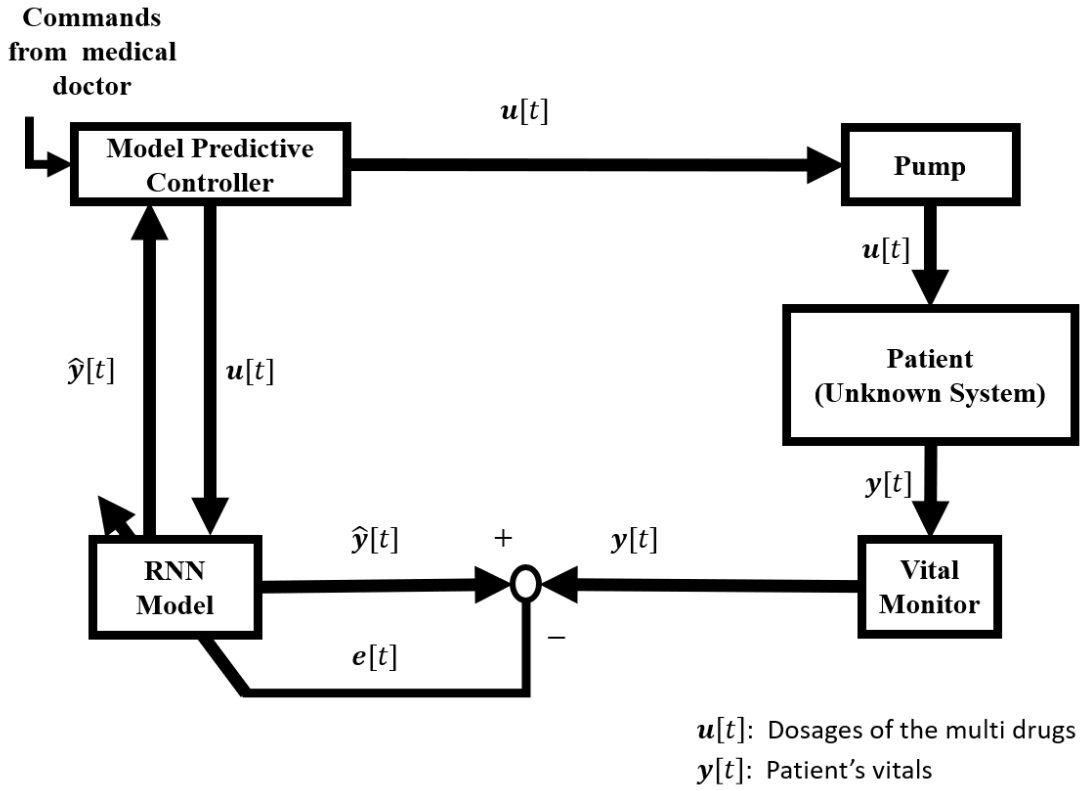

Figure 3.1 The block diagram of the proposed system

The aim of the system is to predict an drug effects and optimize drug dosages based on the prediction. In this paper, the estimation aspect of the system is focused, in which drug dosages $\boldsymbol{u}[t]$ are optimized in each time t. The prediction

is based on estimator using RNN model. Specifically, the medication response to the human body is regarded as an unknown system, and the system is identified by RNN. Moreover, the network parameters were updated using training data, $\boldsymbol{y}[t]$(vital values sensed from the patient).

In next chapter, the overview dependable learning scheme of drug dosage model using RNN and the estimation scheme of the vital behavior are explained.

Chapter 4

Dependable learning scheme of model for predicting drug dosage effect using RNN

4.1 Prediction model using recurrent neural networks

In this subsection, our proposed RNN model for predicting the vital behavior is described. Figure 4.1 shows the structure of the RNN.

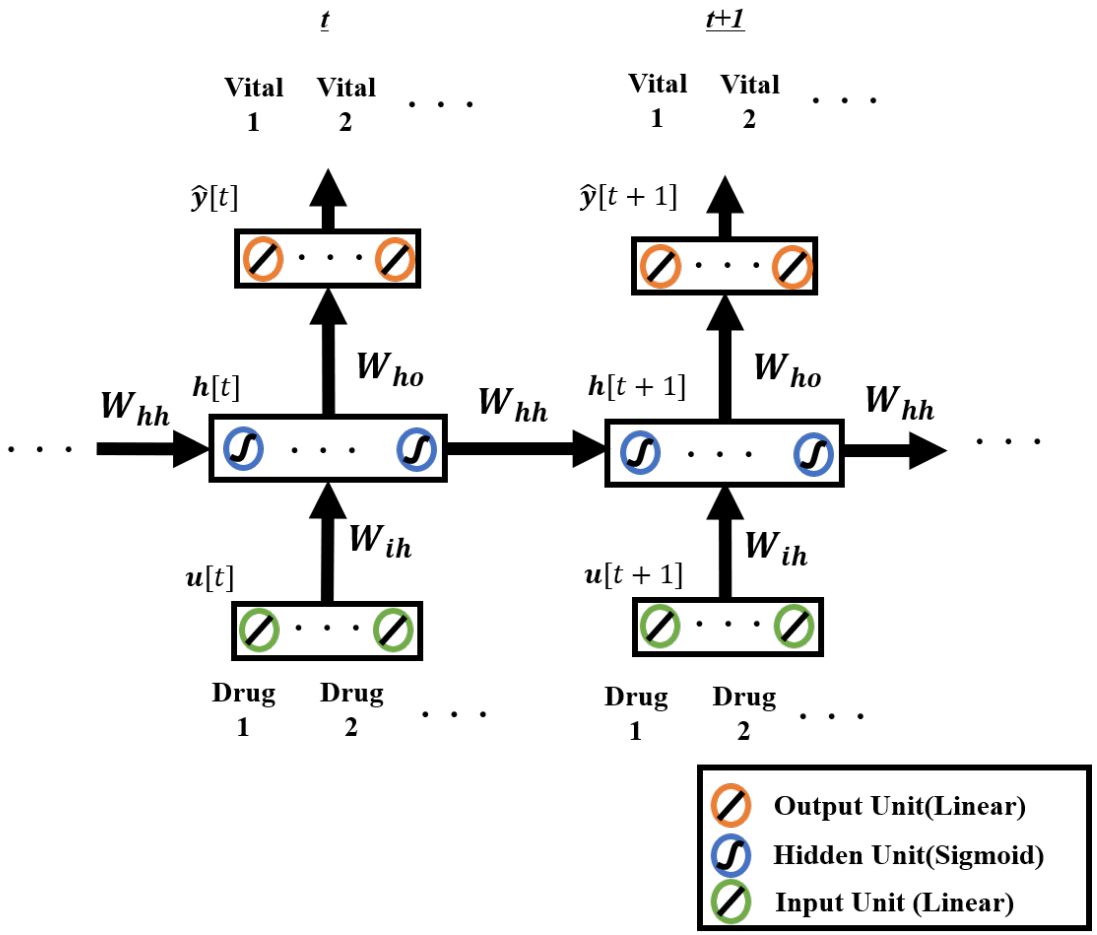

Figure 4.1 RNN model

In our proposed system drug dosages in each time $\boldsymbol{u}[t]$ served as input to the RNN. In the hidden layer, it is assumed that the time variance of the drug absorption in the human body is expressed as the feature of nodes. When applying a neural network to a regression problem, the sigmoid function is generally used for the hidden layer, so the following sigmoid function $\sigma(x)$ was also applied in this study:

$$\sigma(x) = \frac{1}{1 + e^{-x}}. \tag{4–1}$$

Here, the hidden layer output $\boldsymbol{h}[t]$ at time t is expressed as follows:

$$\boldsymbol{h}[t] = \sigma(\boldsymbol{W}_{hh}\boldsymbol{h}[t-1] + \boldsymbol{W}_{ih}\boldsymbol{u}[t]), \tag{4–2}$$

where, $\boldsymbol{W}_{ih}$ is a matrix that summarizes the weights of edges that connect the input layer to the hidden layer, and $\boldsymbol{W}_{hh}$ is a matrix that summarizes the weights of edges that connect the hidden layer of time $t-1$ to the hidden layer of time

t. In addition, since output linearity is commonly used in regression problems, linear output neurons were applied in this study as well. The estimated vital $\hat{\boldsymbol{y}}[t]$, which is the output of the RNN model, is expressed as follows:

$$\hat{\boldsymbol{y}}[t] = \boldsymbol{W_{ho}}\boldsymbol{h}[t], \tag{4–3}$$

where, $\boldsymbol{W_{ho}}$ is a matrix that summarizes the weights of the edge that connect the hidden layer to the output layer.

These weight parameters were updated in our RNN model by the learning algorithm.

4.2 Process flow of the proposed system

Figure 4.2 shows the flowchart of our proposed system.

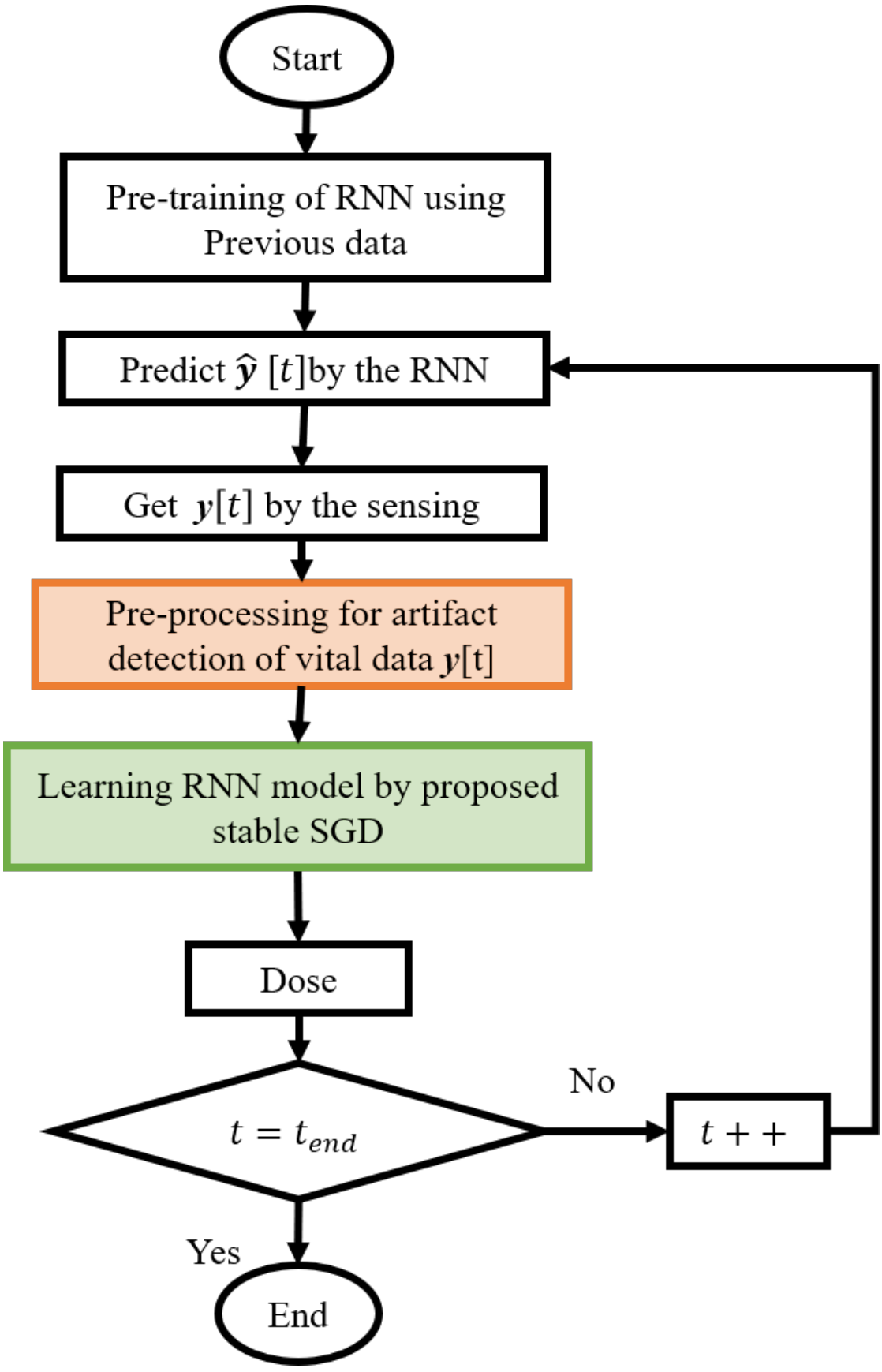

Figure 4.2 Flowchart of the proposed scheme

The t_{end} denotes the end time of the dosing period. In this flowchart, each vital values $\boldsymbol{y}[t]$ is sensed from patients and used to update RNN model in each time step.

In each step time, weights in the RNN model are updated using learning algorithm.

In general, weights in the RNN are updated by stochastic gradient descent (SGD) [29, 30] algorithm. In the SGD algorithm, the weights of the Neural Network are updated to minimize the value of evaluation function. The evaluation function $E[t]$ in each time step is defined as square error between the training data $\boldsymbol{y}[t]$ and the output of the RNN model $\hat{\boldsymbol{y}}[t]$ in order to minimize the prediction error of BIS value. Hence, the function $E[t]$ is defined as follows:

$$E[t] = \frac{1}{2}||\boldsymbol{y}[t] - \hat{\boldsymbol{y}}[t]||^2. \tag{4–4}$$

Using the evaluate function in (4–4),Here, let $\mathbb{W}$ be the set of weights in the RNN. The weighting factor $w_i(i = 1, 2, \cdots, N(\mathbb{W}))$ is updated as follows:

$$w_i[t+1] = w_i[t] - \mu_i \frac{\partial E[t]}{\partial w_i[t]}, \tag{4–5}$$

where, μ_i denotes learning rate for each weight, and $\frac{\partial E[t]}{\partial w_i[t]}$ is partial derivative of $E[t]$ with respect to $w_i[t]$. Based on (4–5), weights $w_i[t]$ are updated sequentially to minimize evaluate function $E[t]$ while the learning of the RNN model proceeds. However, learning performance depends on the value of the learning rate μ_i. When the learning rate μ_i is too small, the speed to improve the estimation accuracy by the RNN becomes slow. When the learning rate μ_i is too large, convergence stability and estimation accuracy using the RNN model cannot be guaranteed. Therefore, it is analyzed that the stability of learning theoretically and proposed stable learning scheme using an optimum learning rate μ_i based on the analysis. In the Chap. 5, the stability analysis and proposed learning algorithm is described in detail.

Another problem is that the data obtained at each step time may contain measurement errors and other vital artifacts. If the data with the artifact is used to train the RNN model, there is a risk that the prediction accuracy of the model will decrease. Therefore, to improve the reliability of the prediction results by the model, pre-processing method to detect artifact before learning the RNN. The details of this method are described in Chap. 6 below.

Chapter 5

Dependable Learning Algorithm based on Lyapunov Stability Theory

5.1 Overview of the proposed algorithm

This chapter describes an online learning method that improves SGD[29, 30]. First, normal SGD always uses a constant learning rate, but as mentioned in Chapter 3, the RNN output becomes unstable depending on the value. Therefore, in the proposed method, the optimum learning rate for each weighting coefficient is first obtained based on the Lyapunov analysis[27, 28], which is an analysis method for nonlinear systems, and a stable learning method using it is proposed. The theoretical analysis of the optimal learning rate will be described in the next chapter.

5.2 Theoretical analysis and optimum learning rate

In this section, the stability of the learning algorithm is analysed based on Lyapunov analysis [27, 28]. The Lyapunov analysis is used to analyze the stability of systems based on the Lyapunov function $L(t)$. From the Lyapunov's stability theorem, if the nonlinear function $L(t)$ is positive-definite and the time derivative of the function $\dot{L}(t)$ takes negative value, the system became stable. In the discrete-time system, the differential of Lyapunov function $\Delta L[t] = L[t+1] - L[t]$ is used to analyze the stability. Here, the condition that the square error between the RNN output and the true value asymptotically converges to 0 is analysed. Moreover, since the squared error is a positive-definite function that is 0 at the origin and takes a positive value otherwise, it can be analyzed as a Lyapunov function. Thus, the evaluation function $E[t]$ is applied as Lyapunov

function for the stability analysis in our RNN model. The error between training data $\boldsymbol{y}[t]$ and the output of the RNN model $\hat{\boldsymbol{y}}[t]$ are expressed as:

$$\boldsymbol{e}[t] = \boldsymbol{y}[t] - \hat{\boldsymbol{y}}[t], \tag{5–1}$$

the Lyapunov function $L[t]$ can be expressed as

$$L[t] = \frac{1}{2}||\boldsymbol{e}[t]||^2. \tag{5–2}$$

From (5–1) and (5–2), time differential of Lyapunov function $\Delta L[t] = L[t+1] - L[t]$ can be expressed as

$$\begin{aligned}
\Delta L[t] &= L[t+1] - L[t] \\
&= \frac{1}{2}(||\boldsymbol{e}[t+1]||^2 - ||\boldsymbol{e}[t]||^2) \\
&= \frac{1}{2}(||\boldsymbol{e}[t] + \Delta\boldsymbol{e}[t]||^2 - ||\boldsymbol{e}[t]||^2) \\
&= \Delta\boldsymbol{e}[t]^T(\boldsymbol{e}[t] + \frac{1}{2}\Delta\boldsymbol{e}[t])
\end{aligned} \tag{5–3}$$

where, $\Delta\boldsymbol{e}[t] = \boldsymbol{e}[t+1] - \boldsymbol{e}[t]$ denotes the differential of error in each time step. Using partial derivative $\frac{\partial \boldsymbol{e}[t]}{\partial w_i[t]}$ and (4–5), $\Delta\boldsymbol{e}[t]$ can be also expressed as

$$\begin{aligned}
\Delta\boldsymbol{e}[t] &= \sum_{i=1}^{N}(\frac{\partial\boldsymbol{e}[t]}{\partial w_i[t]})(w_i[t+1] - w_i[t]). \\
&= \sum_{i=1}^{N}(\frac{\partial\boldsymbol{e}[t]}{\partial w_i[t]})(w_i[t] - \mu_i\frac{\partial E[t]}{\partial w_i[t]} - w_i[t]) \\
&= -\sum_{i=1}^{N}(\frac{\partial\boldsymbol{e}[t]}{\partial w_i[t]})(\frac{\partial E[t]}{\partial w_i[t]}),
\end{aligned} \tag{5–4}$$

where, N denotes the number of weights in RNN. Here, the relationship between partial differential $\frac{\partial E[t]}{\partial w_i[t]}$ and $\frac{\partial \boldsymbol{e}[t]}{\partial w_i[t]}$ can be expressed as

$$\frac{\partial E[t]}{\partial w_i[t]} = \boldsymbol{e}[t]^T\frac{\partial\boldsymbol{e}[t]}{\partial w_i[t]} \tag{5–5}$$

From (5–4) and (5–5), supposing $\boldsymbol{e}[t] \neq \boldsymbol{0}$, the differential $\Delta\boldsymbol{e}[t]$ can be re-written as

$$\begin{aligned}
\Delta\boldsymbol{e}[t] &= \sum_{i=1}^{N}\frac{\mu_i}{||\boldsymbol{e}[t]||^2}\boldsymbol{e}[t](\frac{\partial E[t]}{\partial w_i[t]})^2 \\
&= \frac{\mu_i}{||\boldsymbol{e}[t]||^2}\boldsymbol{e}[t]\sum_{i=1}^{N}\mu_i||\frac{\partial E[t]}{\partial w_i[t]}||^2 \\
&= \frac{\mu_i}{||\boldsymbol{e}[t]||^2}\boldsymbol{e}[t]\boldsymbol{q}^T\boldsymbol{\mu}
\end{aligned} \tag{5–6}$$

where, $\boldsymbol{q} = [||\frac{\partial E[t]}{\partial w_1[t]}||^2, ||\frac{\partial E[t]}{\partial w_2[t]}||^2, \cdots, ||\frac{\partial E[t]}{\partial w_N[t]}||^2]^T$, $\boldsymbol{\mu} = [\mu_1, \mu_2, \cdots, \mu_N]^T$ respectively. From (5–6) and (5–3), the differential of the Lyapunov function $\Delta L[t] = L[t+1] - L[t]$ can be re-written as

$$\begin{aligned}\Delta L[t] &= -\frac{1}{||\boldsymbol{e}[t]||^2}\boldsymbol{e}[t]^T\boldsymbol{q}^T\boldsymbol{\mu}(\boldsymbol{e}[t] - \frac{1}{2}\frac{1}{||\boldsymbol{e}[t]||^2}\boldsymbol{e}[t]\boldsymbol{q}^T\boldsymbol{\mu}) \\ &= -\frac{1}{||\boldsymbol{e}[t]||^2}\boldsymbol{q}^T\boldsymbol{\mu}[||\boldsymbol{e}[t]||^2 - \frac{1}{2}\boldsymbol{q}^T\boldsymbol{\mu}] \\ &= \frac{1}{4E[t]}\boldsymbol{q}^T\boldsymbol{\mu}(\boldsymbol{q}^T\boldsymbol{\mu} - 4E[t]). \end{aligned} \tag{5–7}$$

Therefore, from (5–7), the condition to guarantee stability of the RNN can be expressed as

$$0 \leq \boldsymbol{q}^T\boldsymbol{\mu} \leq 4E[t]. \tag{5–8}$$

While, when the value o $\boldsymbol{q}^T\boldsymbol{\mu}$ take the upper bound of (5–7) the following formula is established:

$$\boldsymbol{q}^T\boldsymbol{\mu} = 4E[t]. \tag{5–9}$$

Then, solving the formula (5–9), the optimum learning rate $\boldsymbol{\mu}^*$ can be expressed as follows:

$$\boldsymbol{\mu}^* = \frac{4E[t]}{||\boldsymbol{q}||^2}\boldsymbol{q}. \tag{5–10}$$

In this paper, learning rate $\boldsymbol{\mu}$ is updated adaptively based on (5–10).

5.3 Performance evaluation

5.3.1 Simulation conditions

In this section, some evaluations to confirm the prediction accuracy of our proposal are performed. Here, assuming the administration of anesthesia to the patient during surgery, the estimation performance of vitals corresponding to each of the administration of a sedative and an analgesic is evaluated. First, the effectiveness of sedatives is assumed to be assessed using the Bispectral Index (BIS). On the other hand, the effectiveness of analgesics is assumed to be assessed using the pain index(PI) used in the paper[3].

Thus, the BIS and PI behaviors of 12 patients are simulated to evaluate the efficiency of our proposal. To simulate the true BIS value for each patient,

the Schnider and Minto model [19] and response surface model[3] are applied(Details of those models are disrobed in detail in the Appendix.). Also, the parameter sets used in [2] is applied; they are shown in Table 5.1.

Table 5.1 Parameter of the Patient model [2]

Patient ID	Age	Height[cm]	Weight[kg]	Gender
1	74	164	88	Male
2	67	161	69	Male
3	75	176	101	Male
4	69	173	97	Male
5	45	171	64	Male
6	57	182	80	Male
7	74	155	55	Female
8	71	172	78	Male
9	65	176	77	Male
10	72	192	73	Male
11	69	168	84	Female
12	60	190	92	Male

The Dosages in each time step were controlled by the a PID control [37] with an target BIS value of 50 and that of PI value is 4.5 that is applied in[3]. The gain of the PID controller was decided based on Ziegler- Nichols' method [37] that is one of the typical methods to decide the gain. Furthermore, to evaluate the efficiency of our proposed scheme, it is compared that the prediction performance of our proposed scheme with that of the conventional scheme. In the study, proposed scheme is compared with SGD[29, 30], RMSprop[31],and Adam[32] that is the generally used learning algorithm to train neural networks. Table 5.2 shows the simulation parameters.

Table 5.2 simulation parameters

simulation time[min.]	10
Sampling Period T_s[sec.]	2.0
Gain of the PID controller	
Proportional Gain: K_p	0.055
Integral Gain: K_i	0.001
Derivative Gain: K_i	2.68
Target BIS value in the control	50.0
Target PI value in the control	4.5
Parameter for SGD[29, 30] (Conventional)	
Learning rate μ	0.004, 0.04, 0.40
Parameter for RMSprop[31] (Conventional)	
μ	0.004, 0.04, 0.40
β	0.9
ϵ	10^{-8}
Parameter for Adam[32] (Conventional)	
μ	0.004, 0.04, 0.40
β_1	0.9
β_2	0.999
ϵ	10^{-8}
Number of units in hidden layer N (the size of weight vectors)	10
Activation function in hidden layer	Sigmoid
Activation function in output layer	Linear
Number of hidden layers	1

Note that the simulation time indicates the maximum elapsed time since drugs are first administered to the patient in the simulation. Moreover, it is assumed that the sampling period of the BIS and PI value from each monitors to be 2.0 second, which is the same as the BIS monitor used in [1]. The number of units in the hidden layer was decided experimentally. It is evaluated that the estimated vital value and the absolute error between estimated BIS value and the true vital value in each patients. Also, the mean absolute error (MAE) during surgery which denotes the average of absolute error over a period of time is also evaluated. The MAE is defined as follows:

$$MAE_i = \frac{1}{T}\sum_{t=1}^{T} |y_i[t] - \hat{y}_i[t]| \tag{5–11}$$

where T denotes the number of samples. $y_i[t]$ and $\hat{y}_i[t]$ denote the true and estimated vital values. When the index i is 1, $y_i[t]$ and $\hat{y}_i[t]$ corresponds to the BIS value. Similarly, when the index i is 2, $y_i[t]$ and $\hat{y}_i[t]$ corresponds to the PI value.

5.3.2 Numerical results

Comparison between SGD and proposed scheme

Here, the simulation results is described. The MAE of this period is shown in Figure 5.1 and 5.2 .

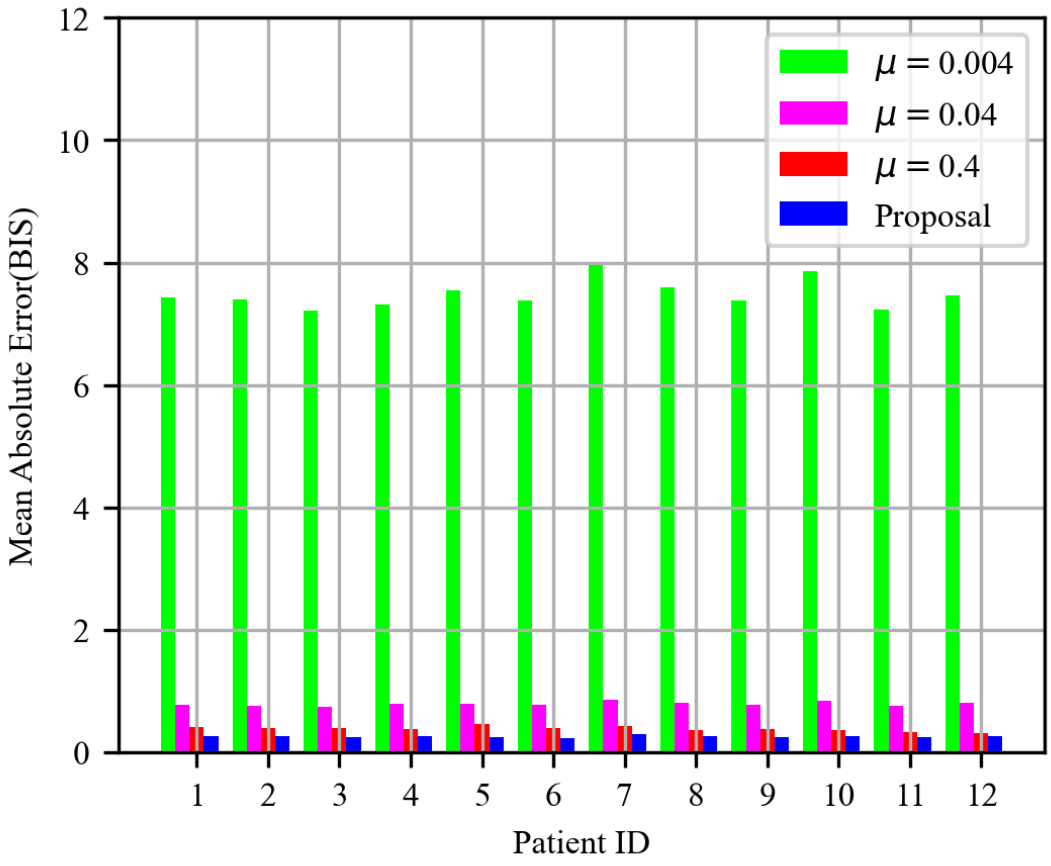

Figure 5.1 Mean Absolute Error in each patient(BIS,Compared with SGD)

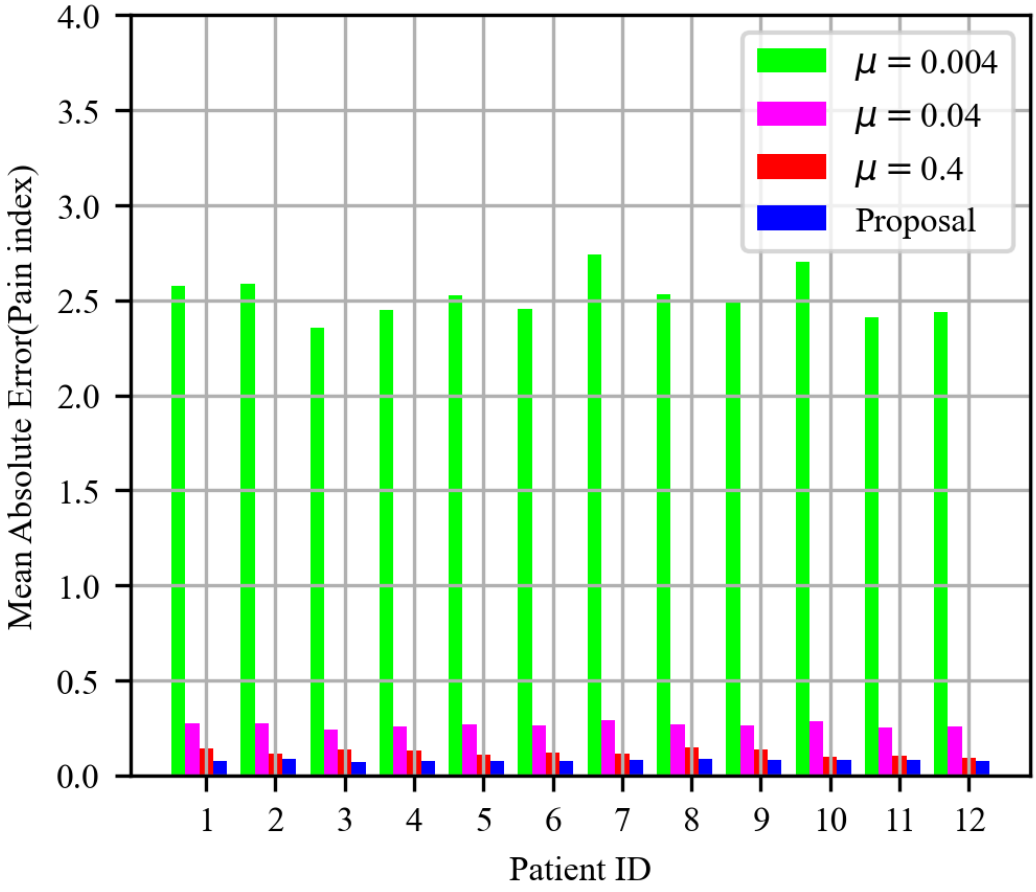

Figure 5.2 Mean Absolute Error in each patient(PI, Compared with SGD)

The MAE values in the proposal are lower than all comparison in all patients. In particular, MAE value in the case learning rate is fixed to 0.004 takes higher compared with other case. Next, the performance evaluation for each patient will be described. Figure 5.3 and 5.4 shows the transition of the BIS value of the Patient 1.

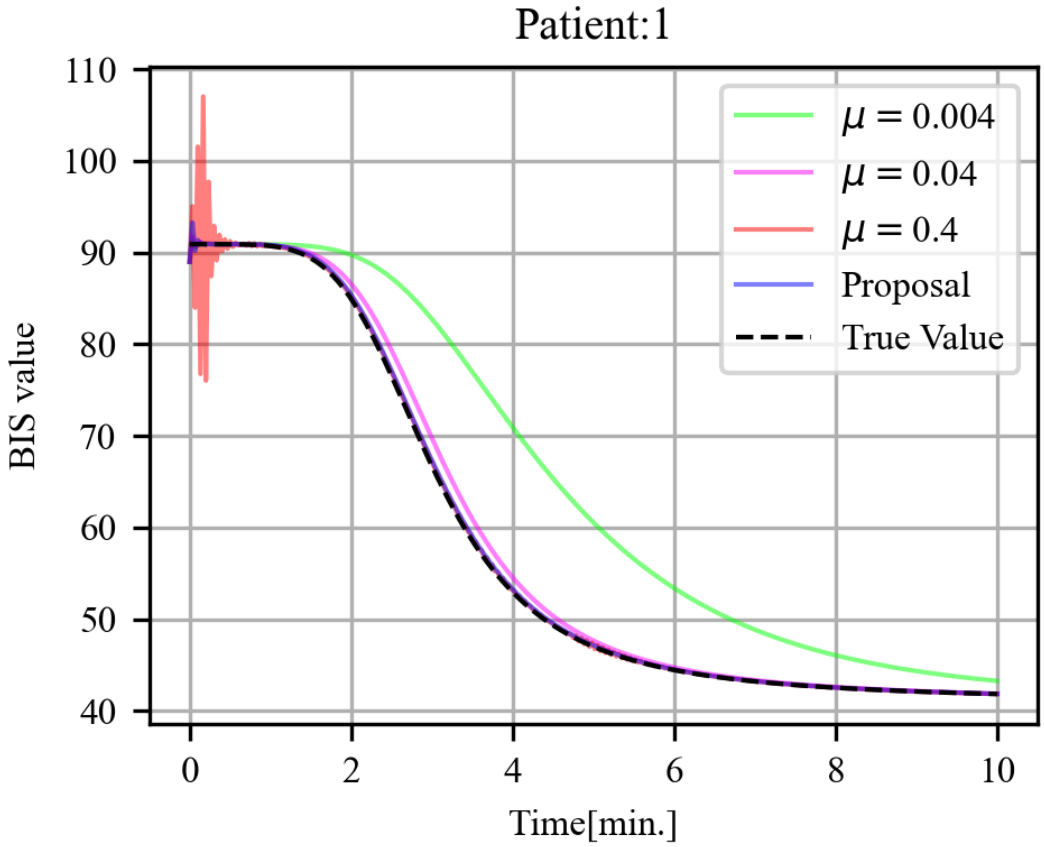

Figure 5.3 Transition of the BIS value in the Patient 1(Compared with SGD)

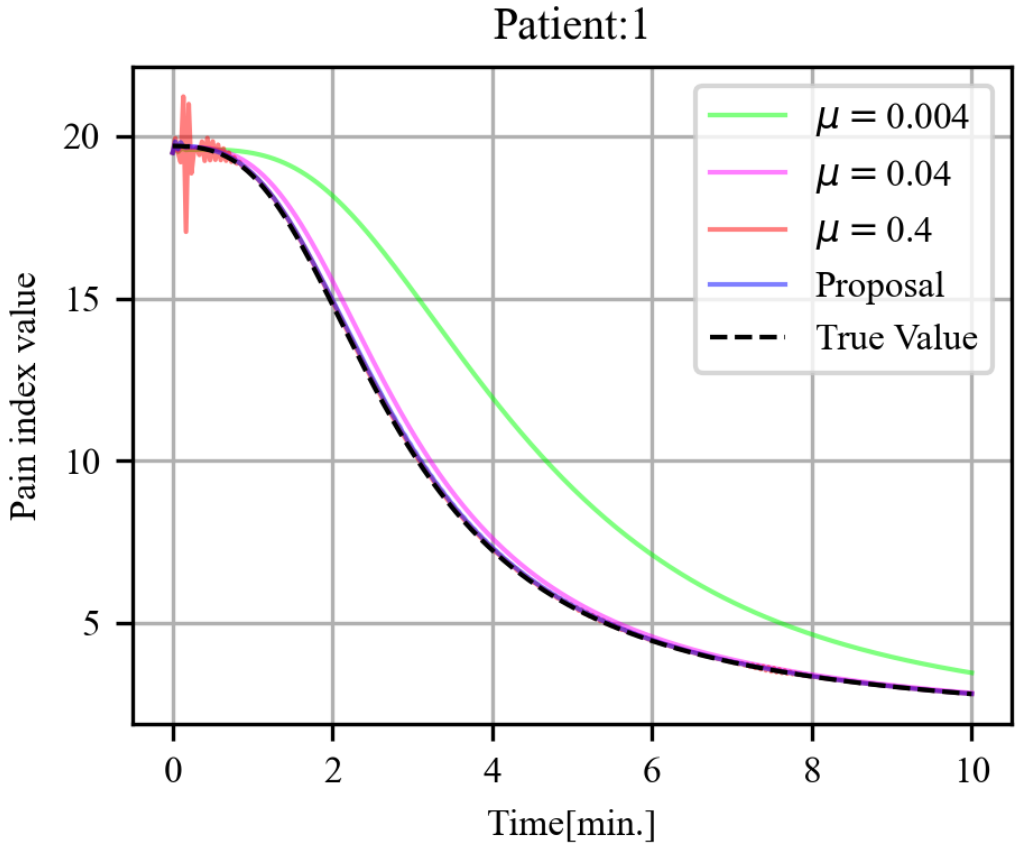

Figure 5.4 Transition of the PI value in the Patient 1(Compared with SGD)

From Fig. 5.3 and 5.4, the estimated BIS and PI value from the proposed scheme(i.e., blue line) seems to be close value to true value in the simulation (i.e., the dotted line) compared to the value in the case learning rate is fixed to 0.004 and 0.04.The estimated BIS and PI values in the case learning rate is fixed to 0.004 and seem to be converged slower compared to the other cases. While, the estimated BIS and PI values in the case learning rate is fixed to 0.4 seem to be converged as fast as proposal. However, it can also be confirmed that the estimated values oscillates in the result when the learning rate is fixed at 0.4 around 1 minute. Especially, estimated BIS value in the case learning rate is fix to 0.4 oscillates from 80 to 110 of BIS. It is unstable output and can be said that it cannot be used as a prediction model.

Figure 5.5 and 5.6 shows the squared error between the estimated BIS and PI values by the RNN model and the true value.

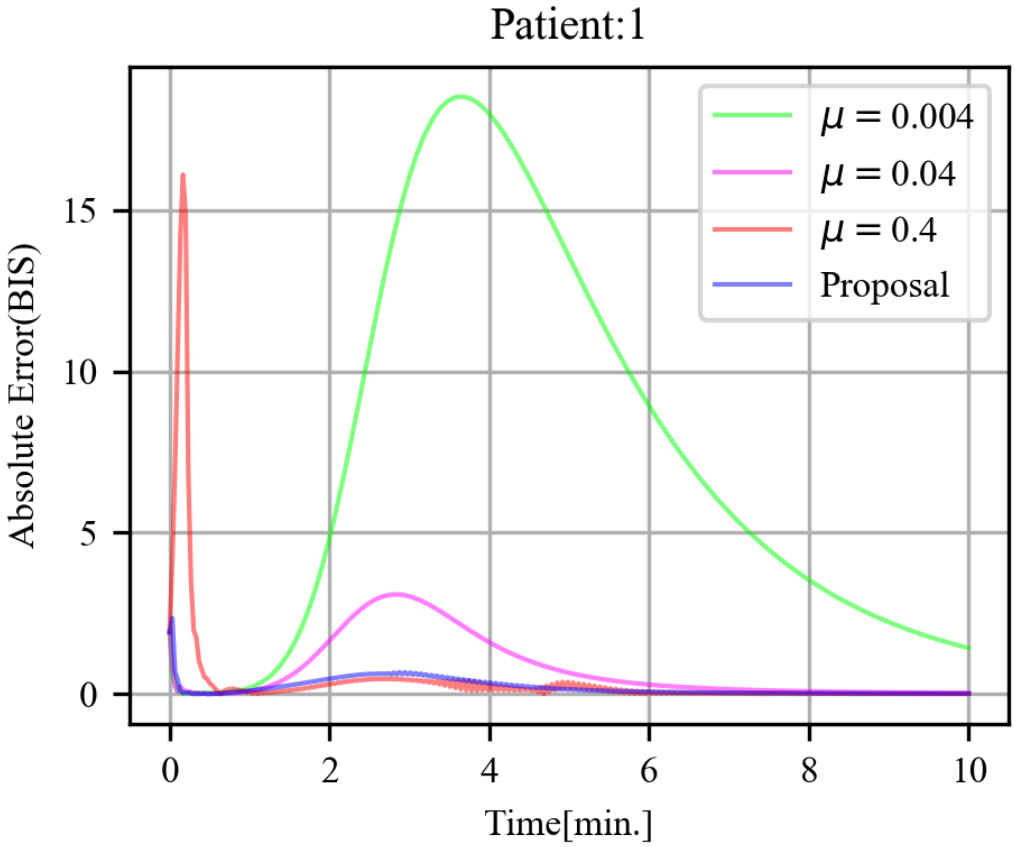

Figure 5.5 Transition of squared error in the Patient 1(BIS,Compared with SGD)

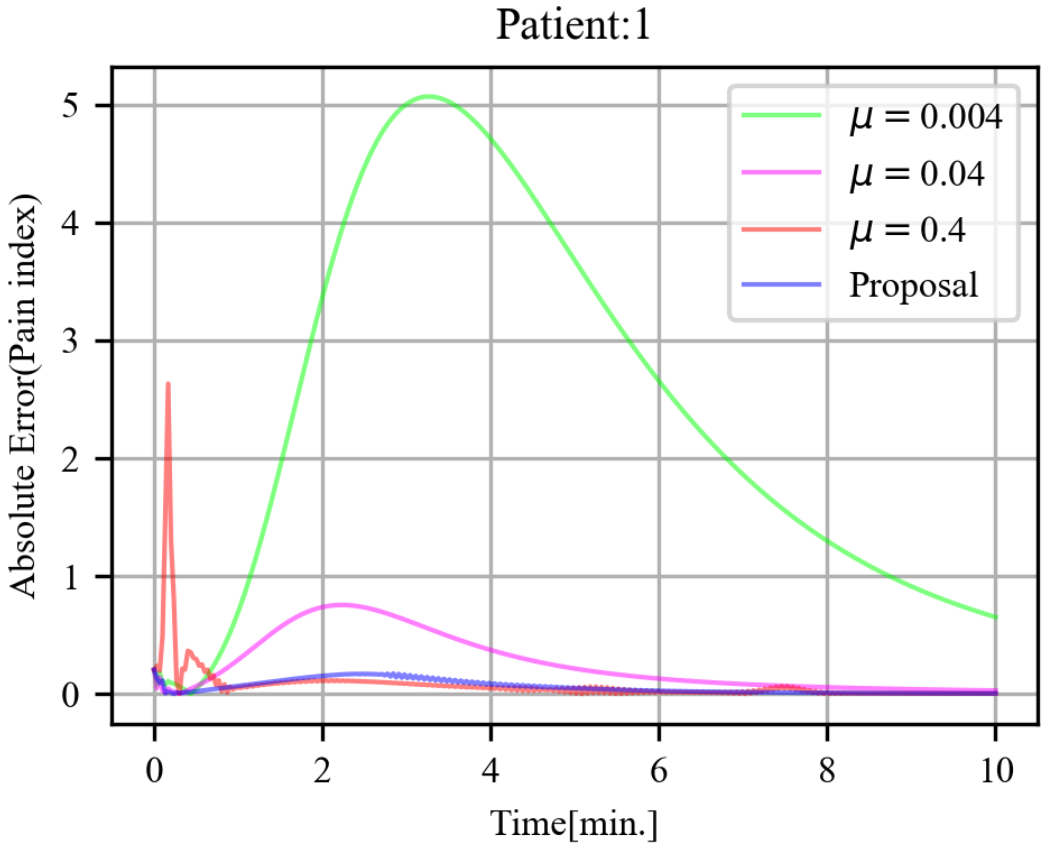

Figure 5.6 Transition of squared error in the Patient 1(PI,Compared with SGD)

From figure 5.5 and 5.6, it is confirmed that the absolute error in the proposal (i.e., the blue line) takes lower than 5.0 and 1.0. Those worst value are lowest value compared with the worst values of all conventional. The absolute error in the case learning rate is fixed to 0.004 sometimes takes higher than 15(BIS) and 5(PI). Also, the absolute error in the case learning rate is fixed to 0.4 takes higher than 15(BIS) and 2(PI) around 1 minute.

From those results, it is confirmed that the efficiency of our proposed scheme compared to the scheme with a fixed learning rate in the worst error.

Next, stability of the in each cases are evaluated. From eq. (5–8), stability index can be defined by following equation:

$$S(\boldsymbol{\mu}) = \frac{4E[t]}{\boldsymbol{q}^T \boldsymbol{\mu}} \tag{5–12}$$

This equation (5–12) shows that the stability of the output cannot be guaranteed when the stability index is 1 or more, but conversely, the stability can be

guaranteed when the stability index is 1 or less. Figure 5.7 shows the transition of the stability index $S(\boldsymbol{\mu})$ in the Patient 11.

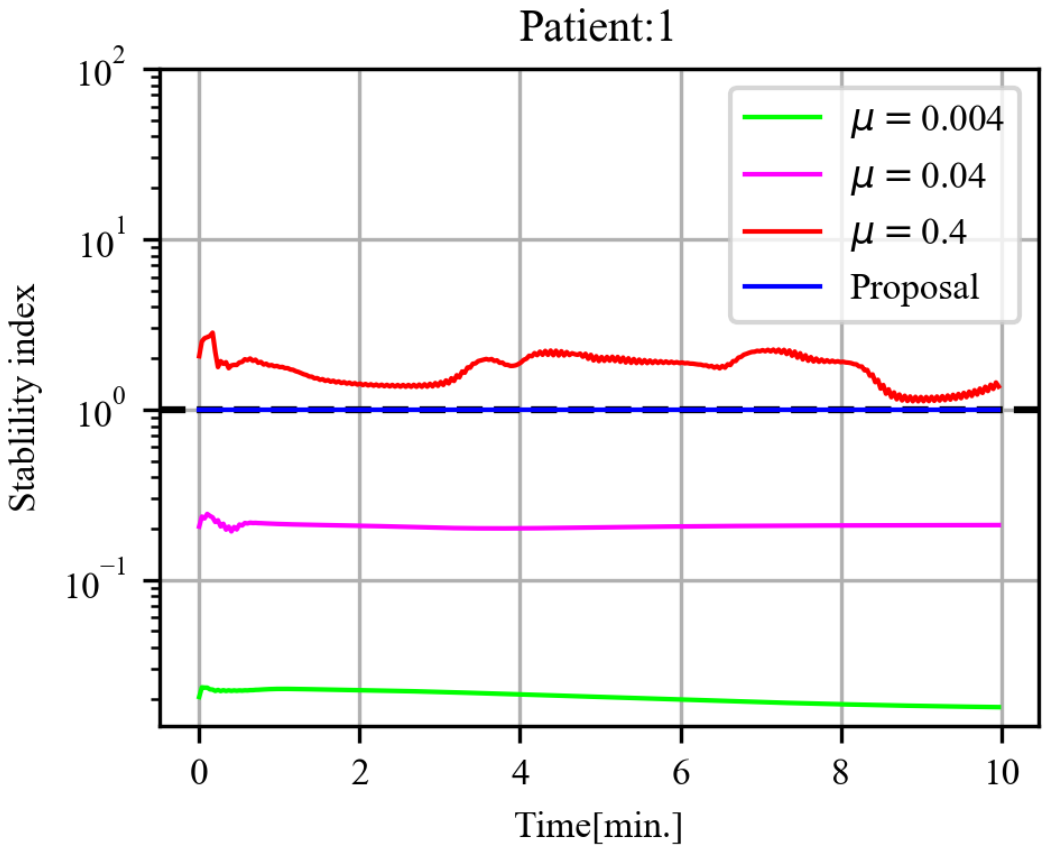

Figure 5.7 Stability index in the Patient 1

From figure 5.7, it can be confirmed that stability index of the proposed scheme takes 1.0. It is the theoretical result.Also, it can be confirmed that the stability in the case learning rate is fixed to 0.4 takes higher than 1.0 and especially takes higher than 2 around the 1 minute. It can be said that this state is far from the region where stability can be guaranteed, and it is considered that the estimated value oscillate significantly in about 1 minute.

Next, fig. 5.8 shows the transition of the power of gradients in the proposed scheme.

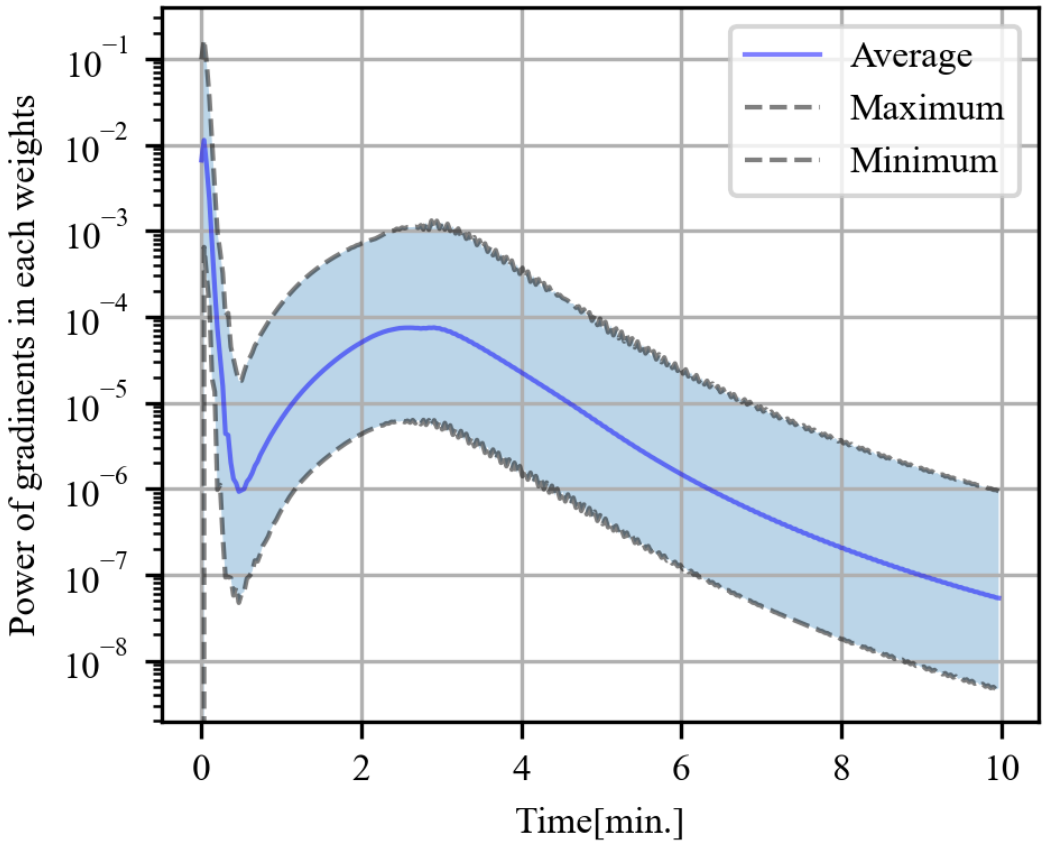

Figure 5.8 Power of gradients in each weights (Patient 1)

From fig. 5.8, it can be confirmed that the average power of gradients takes around 10^{-6} around 1 minutes. However, the average power of gradients become higher around 3 minutes and converged after 3 minutes. From the result of fig. 5.8, it can be considered that the solution of the RNN drops local minimum around one minutes. Therefore, we need to propose the scheme to escape local minimum in the future works.

Comparison between RMSprop and proposed scheme

Here, the comparison between proposed scheme and RMSprop is described. The MAE of this period is shown in Figure 5.9 and 5.10 .

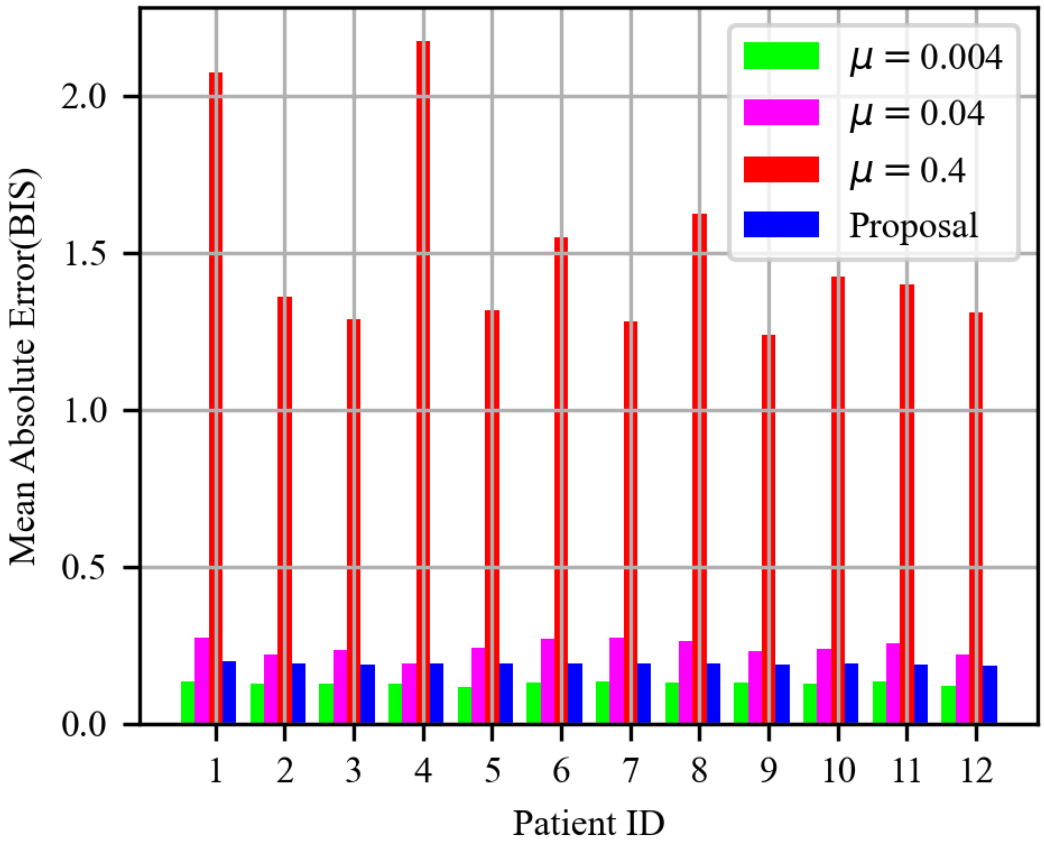

Figure 5.9 Mean Absolute Error in each patient(BIS,Compared with RMSprop)

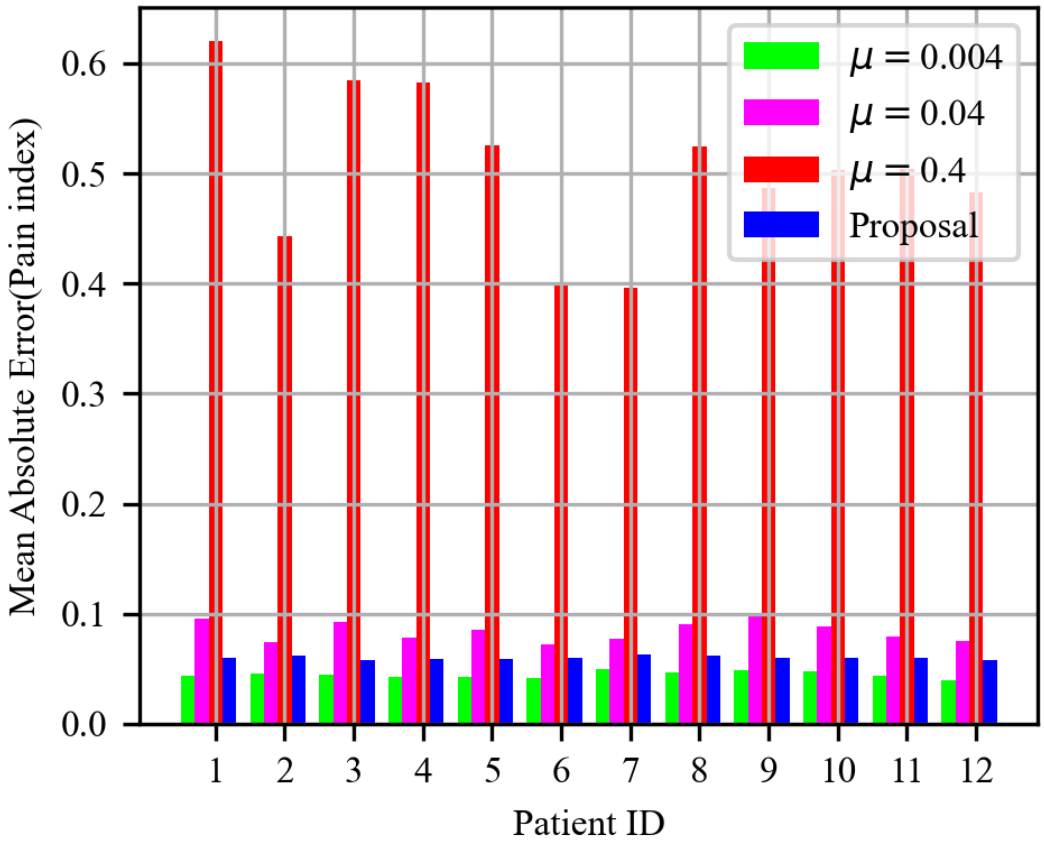

Figure 5.10 Mean Absolute Error in each patient(PI,Compared with RMSprop)

The MAE values in the proposal are lower than comparison in the case the parameter μ is fixed to 0.4 and 0.04 in all patients. In particular, MAE value in the case the parameter μ is fixed to 0.4 takes higher compared with other case. However, the MAE values in the proposal are higher than the conventional in the case the parameter μ is fixed to 0.004 in all patients. Next, the performance evaluation for each patient will be described. Figure 5.11 and 5.12 shows the transition of the BIS and PI value of the Patient 1.

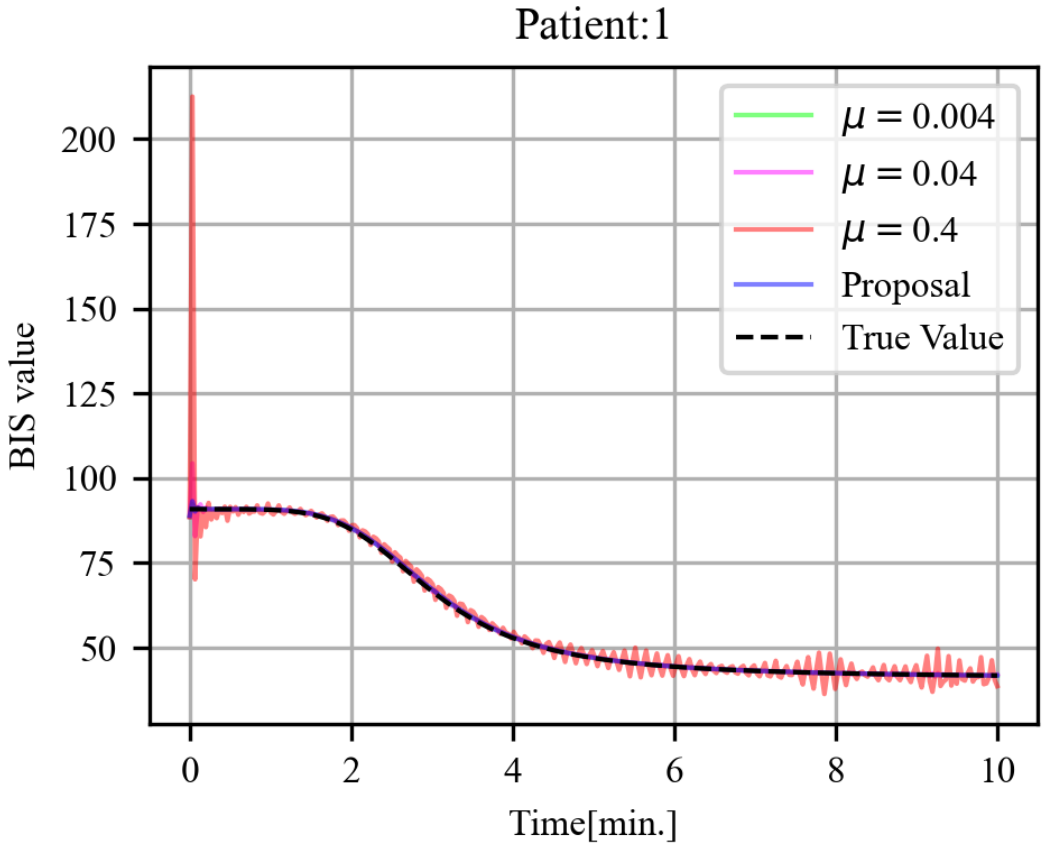

Figure 5.11 Transition of the BIS value in the Patient 1(Compared with RM-Sprop)

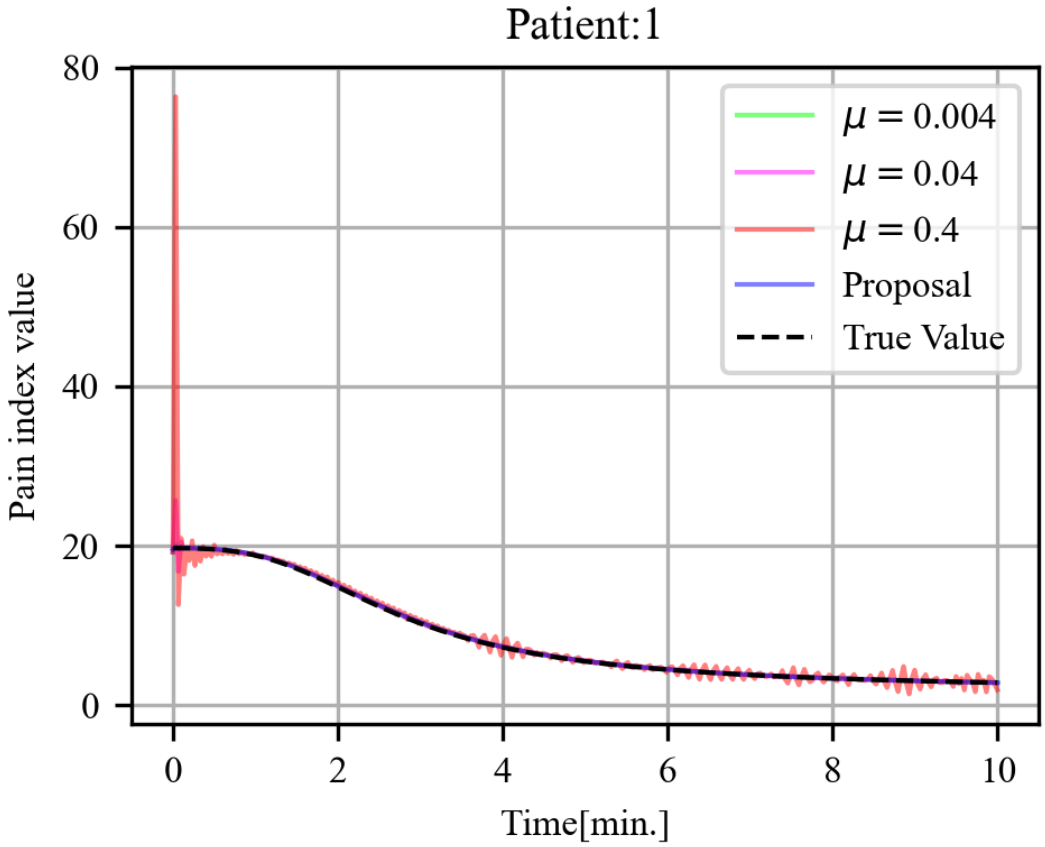

Figure 5.12 Transition of the PI value in the Patient 1(Compared with RMSprop)

From Fig. 5.11 and 5.12, the estimated BIS and PI value from the proposed scheme and all conventional seems to be close value to true value in the simulation (i.e., the dotted line). However, it can also be confirmed that the estimated values oscillates in the result when the parameter μ is fixed at 0.4. In particular, estimated BIS value in the case the parameter μ is fixed to 0.4 oscillates from 75 to 200 of BIS. It is unstable output and can be said that it cannot be used as a prediction model.

Next, fig. 5.13 and 5.14 shows enlarged view of fig. 5.11 and 5.12

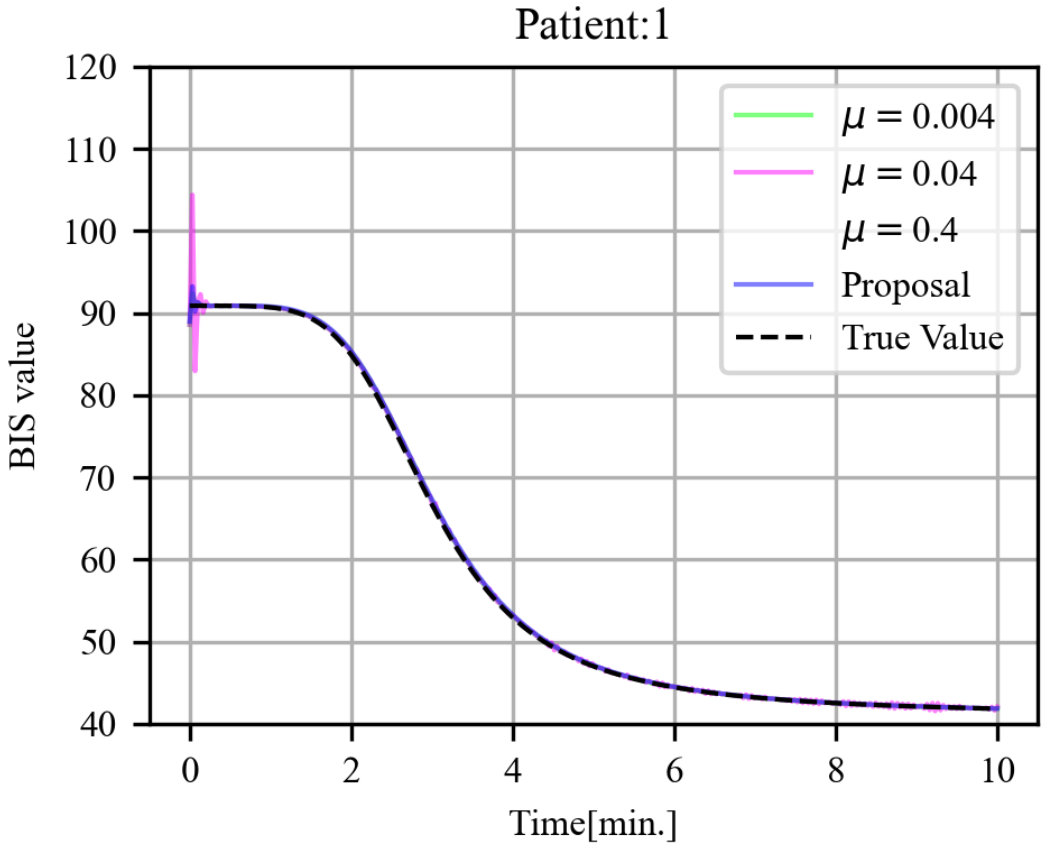

Figure 5.13 Transition of the BIS value in the Patient 1(Compared with RM-Sprop,enlarged view)

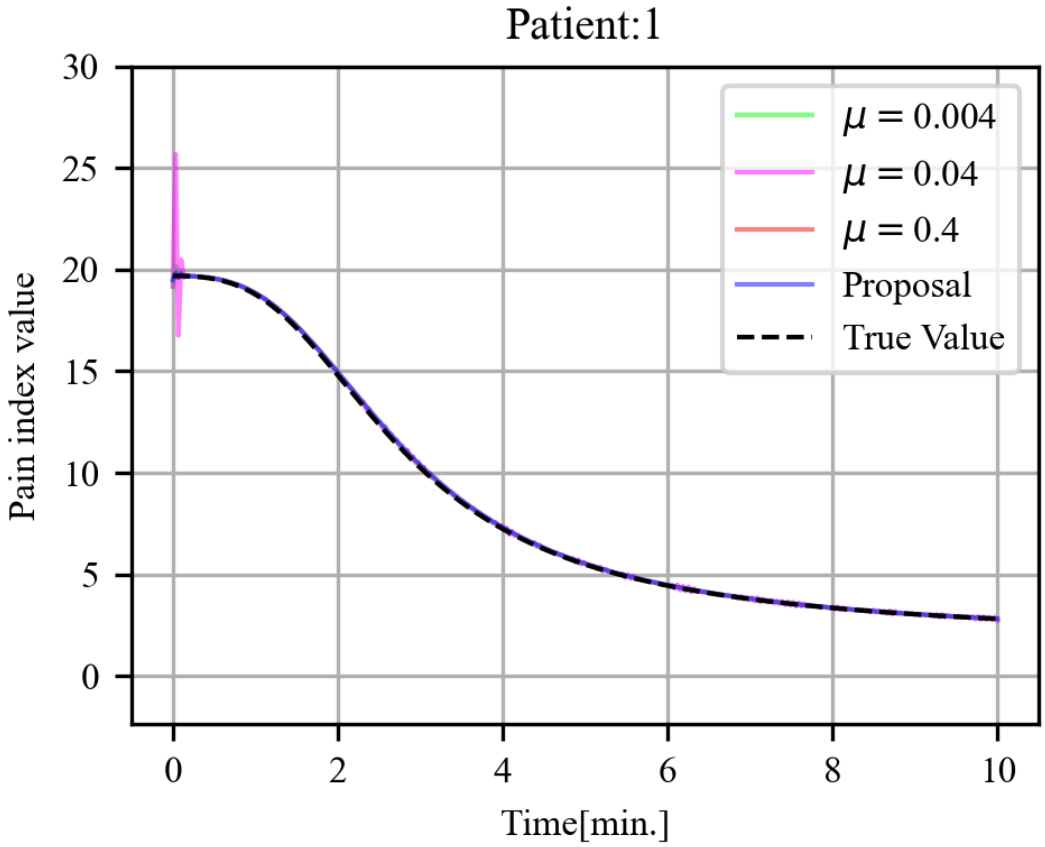

Figure 5.14 Transition of the PI value in the Patient 1(Compared with RMSprop,enlarged view)

From Fig. 5.13 and 5.14, the estimated BIS and PI when the parameter μ is fixed at 0.04 seems oscillates around 1 minutes. Moreover, the estimated BIS and PI when the parameter μ is fixed at 0.004 seems to be similar to those of proposal.

Figure 5.15 and 5.16 shows the squared error between the estimated BIS and PI values by the RNN model and the true value.

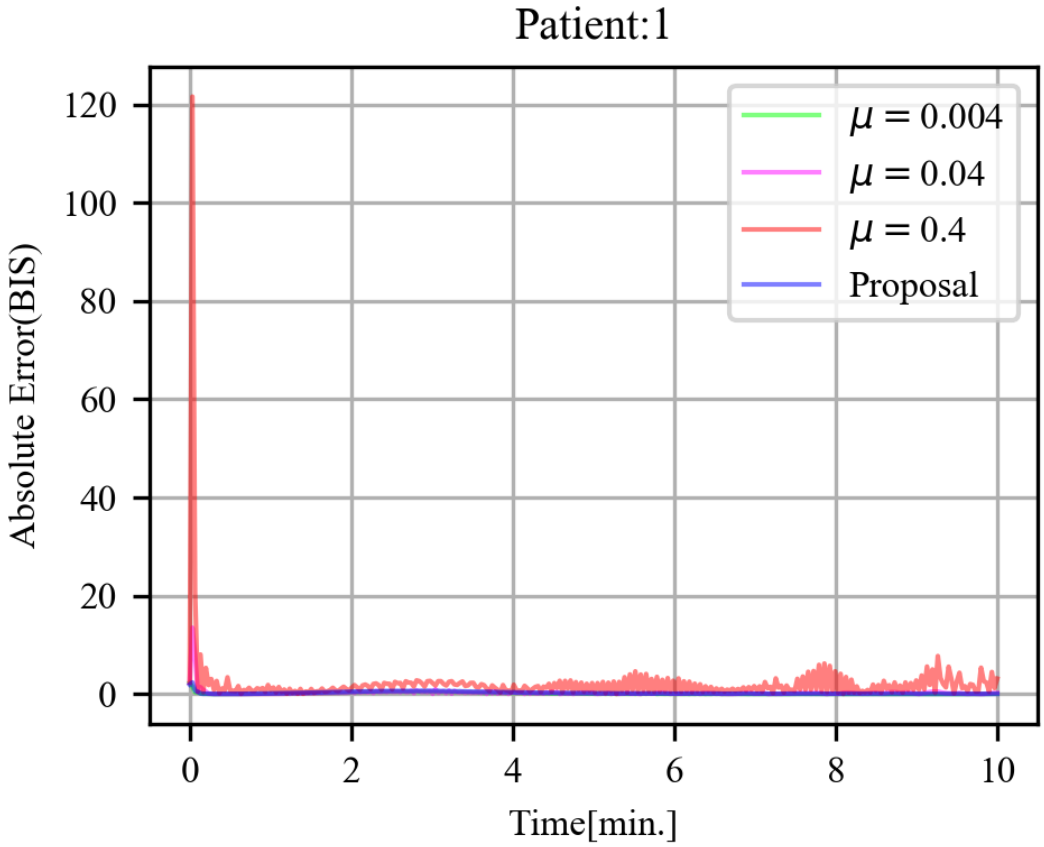

Figure 5.15 Transition of absolute error in the Patient 1(BIS,Compared with RMSprop)

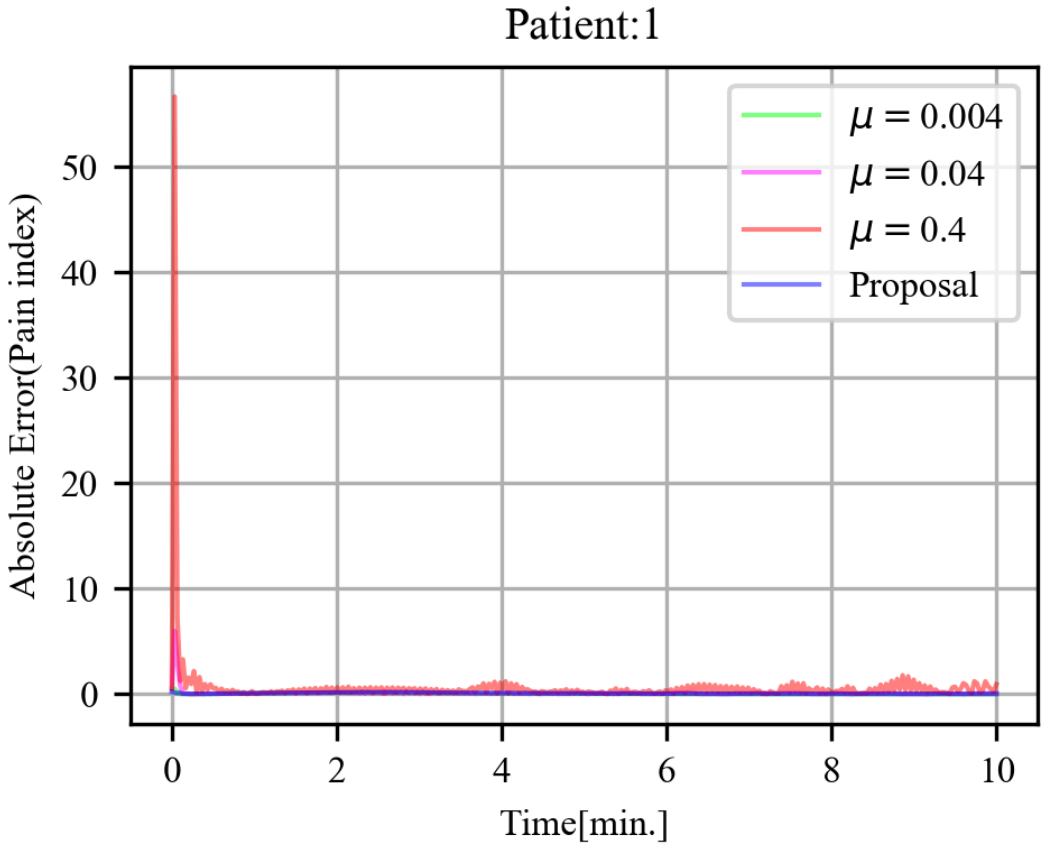

Figure 5.16 Transition of absolute error in the Patient 1(PI,Compared with RMSprop)

From figure 5.15 and 5.16, it is confirmed that the absolute error in the case the parameter μ is fixed to 0.4 takes higher value compared with the other results. Especially, the absolute error takes higher than 120(BIS) and 50(PI) around 1 minute.

Next, fig. 5.17 and 5.18 shows enlarged view of fig. 5.15 and 5.16

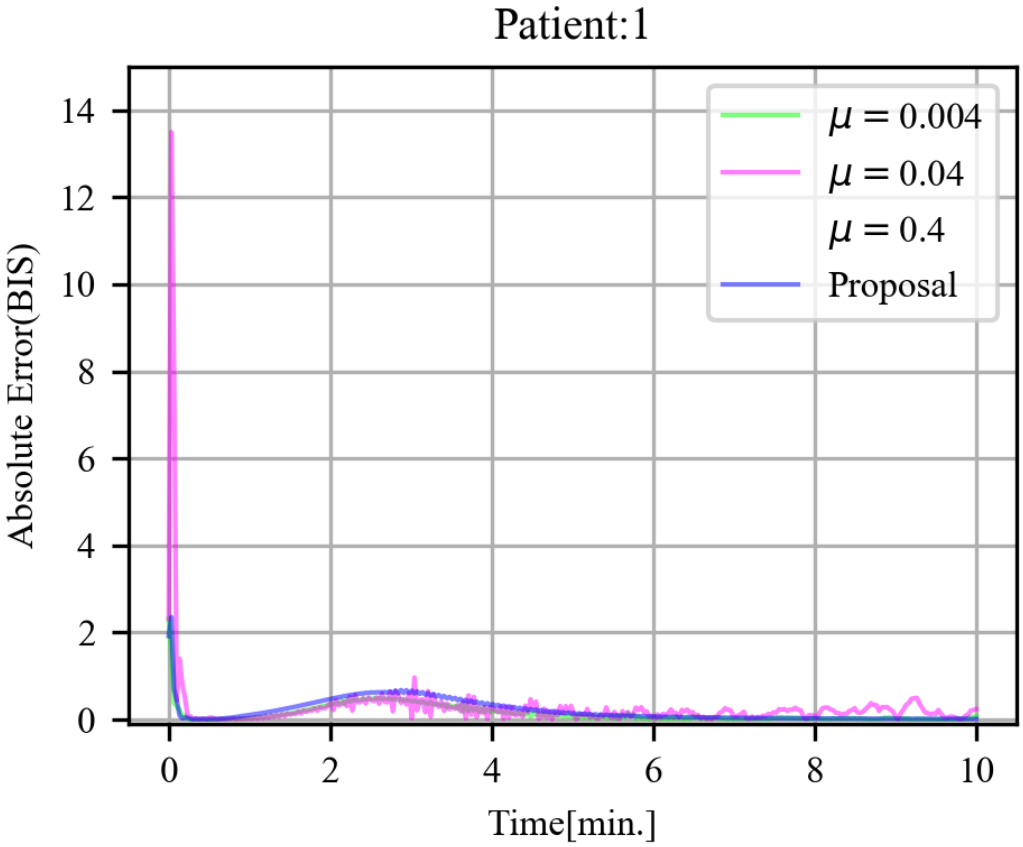

Figure 5.17 Transition of absolute error in the Patient 1(BIS,Compared with RMSprop,enlarged view)

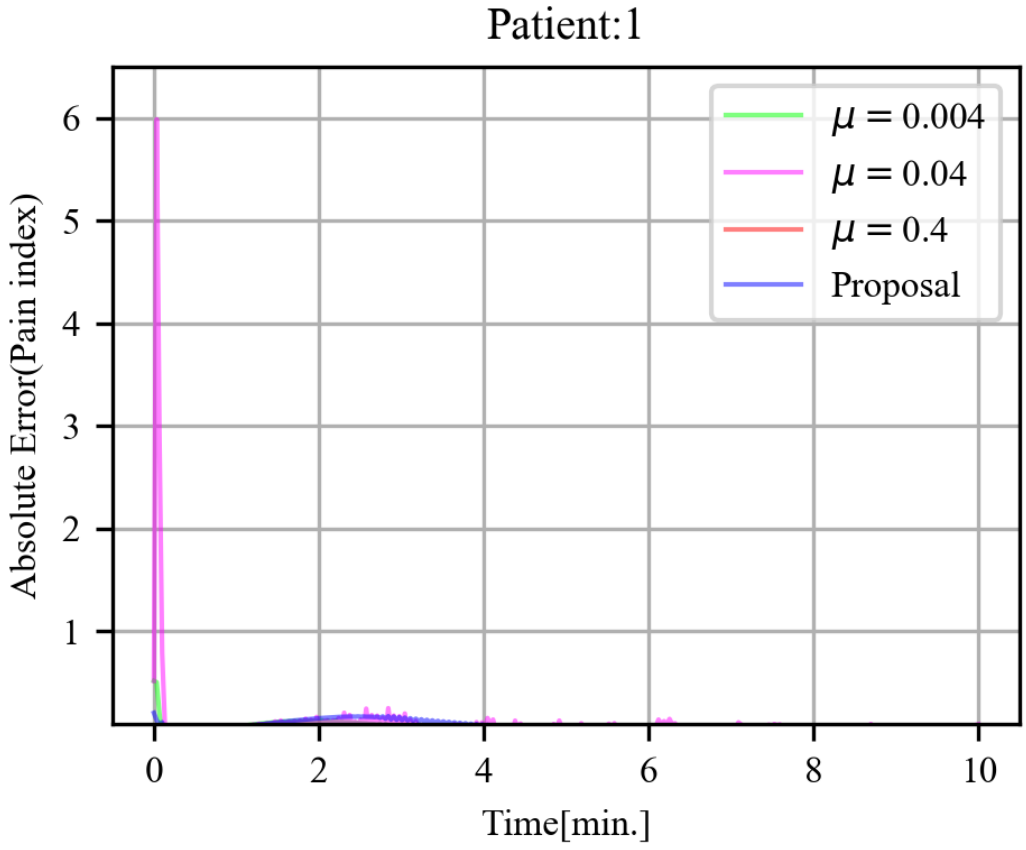

Figure 5.18 Transition of absolute error in the Patient 1(PI,Compared with RMSprop,enlarged view)

From Fig. 5.17 and 5.18, maximum absolute error in each vital when the parameter μ is fixed at 0.04 takes higher than those of proposal.

Moreover, the estimated BIS and PI when the parameter μ is fixed at 0.004 seems to be similar to those of proposal. It is considered that the reason for such a result is that the vital signs started to change suddenly from around 2 minutes, so that the speed of change cannot be followed when online learning is performed at a lower learning rate.

From those results, it is confirmed that the efficiency of our proposed scheme compared to the scheme with a various parameter μ. It was also confirmed that the performance of the proposed method may be almost the same as that of RMSprop depending on the parameter selection.

Comparison between Adam and proposed scheme

Here, the comparison between proposed scheme and Adam is described. The MAE of this period is shown in Figure 5.19 and 5.20 .

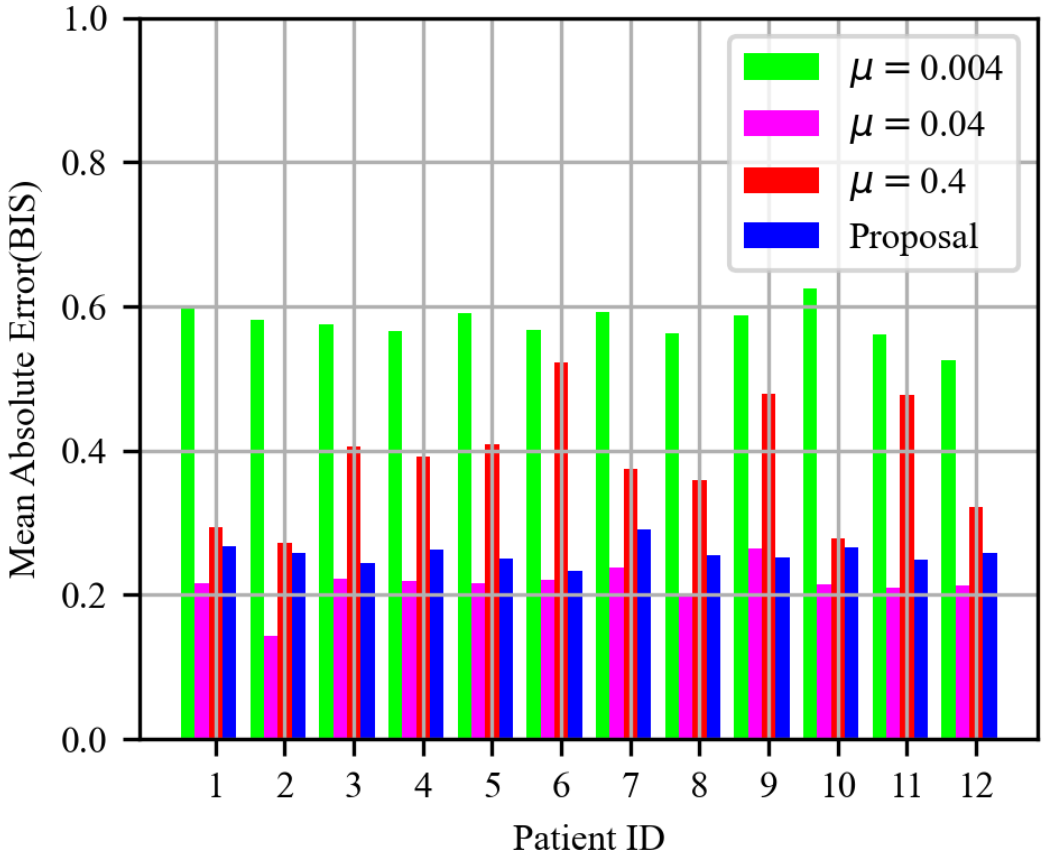

Figure 5.19 Mean Absolute Error in each patient(BIS,Compared with Adam)

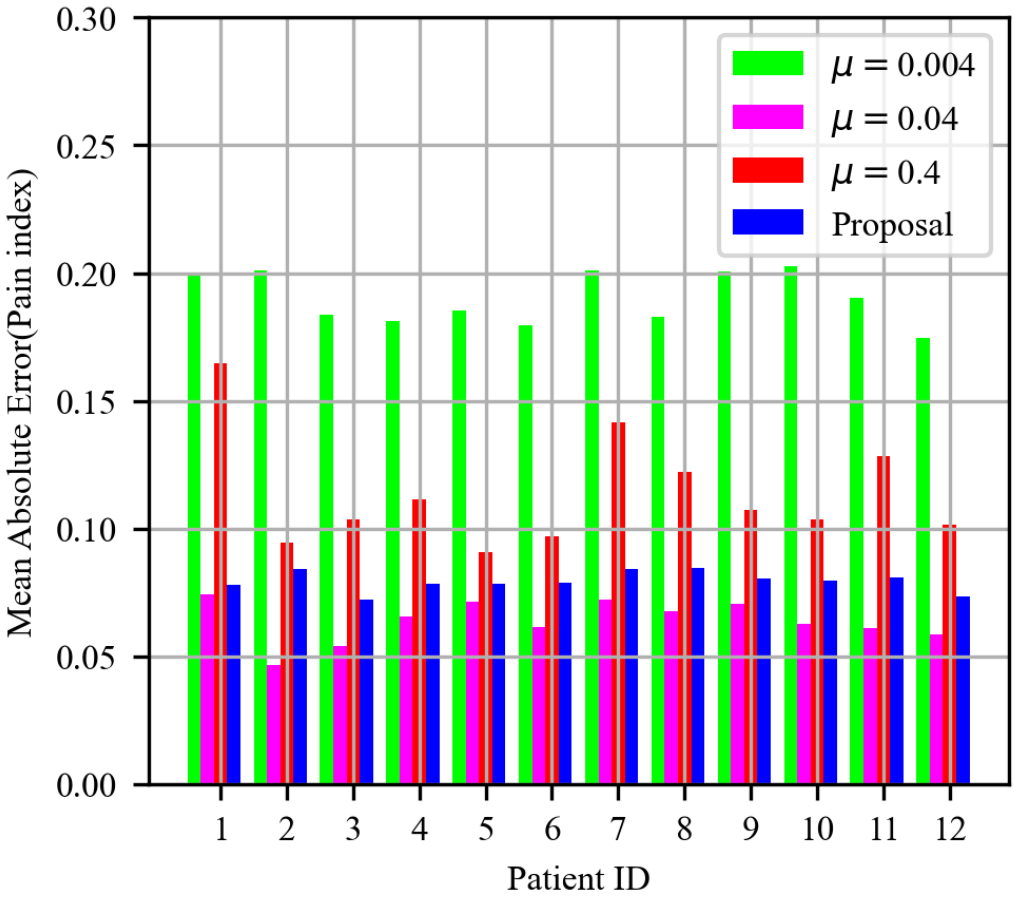

Figure 5.20 Mean Absolute Error in each patient(PI,Compared with Adam)

The MAE values in the proposal take lower than the case the parameter μ is fixed to 0.004 and 0.4 in all patients. In particular, MAE value in the case the parameter μ is fixed to 0.004 takes higher compared with other case. However, The MAE in the case the parameter μ is fixed to 0.04 take lower value compared with proposed scheme.

Next, the performance evaluation for each patient will be described. Figure 5.21 and 5.22 shows the transition of the BIS and PI value of the Patient 1.

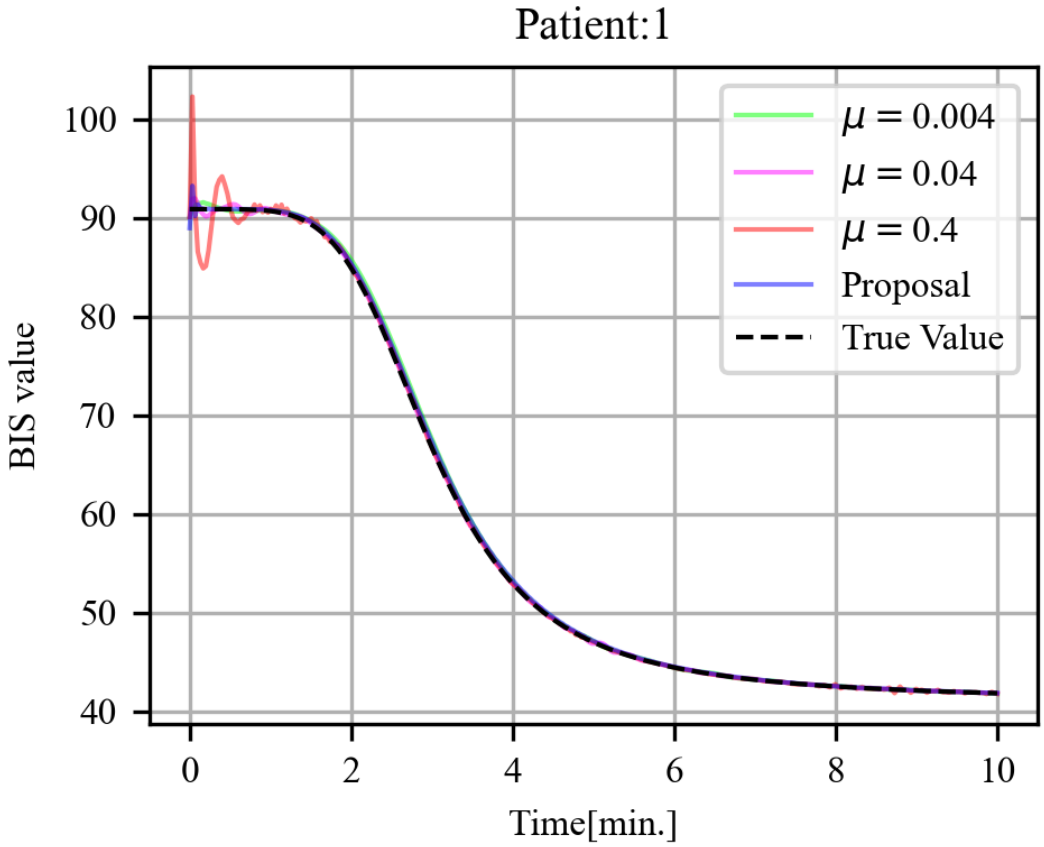

Figure 5.21 Transition of the BIS value in the Patient 1(Compared with Adam)

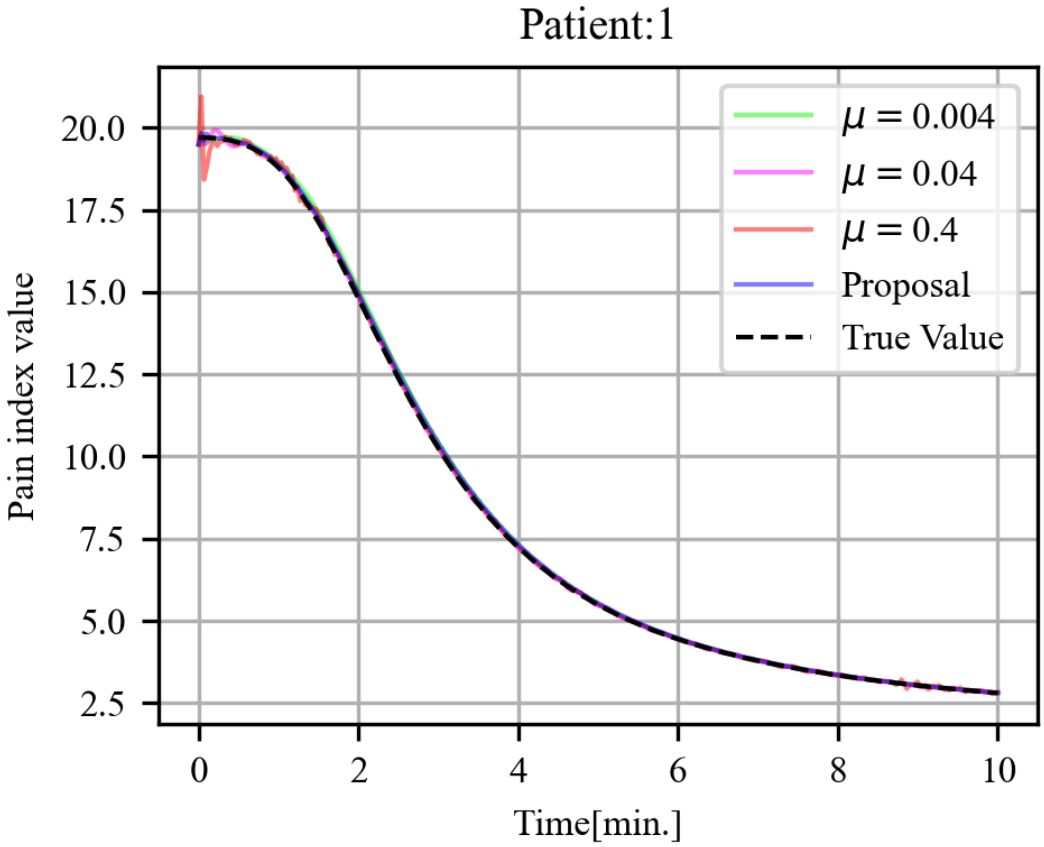

Figure 5.22 Transition of the PI value in the Patient 1(Compared with Adam)

From Fig. 5.21 and 5.22,It can be seen that the estimated BIS and PI value from the proposed scheme and all conventional converge to true value in the simulation (i.e., the dotted line). However, it can also be confirmed that the estimated values oscillates in the result when the parameter μ is fixed at 0.4. In particular, estimated BIS value in the case the parameter μ is fix to 0.4 takes larger than 100 of BIS even though the true value takes around 90. It is unstable output and can be said that it cannot be used as a prediction model.

Next, fig. 5.23 and 5.24 shows enlarged view of fig. 5.21 and 5.22(from 2 to 5 minutes).

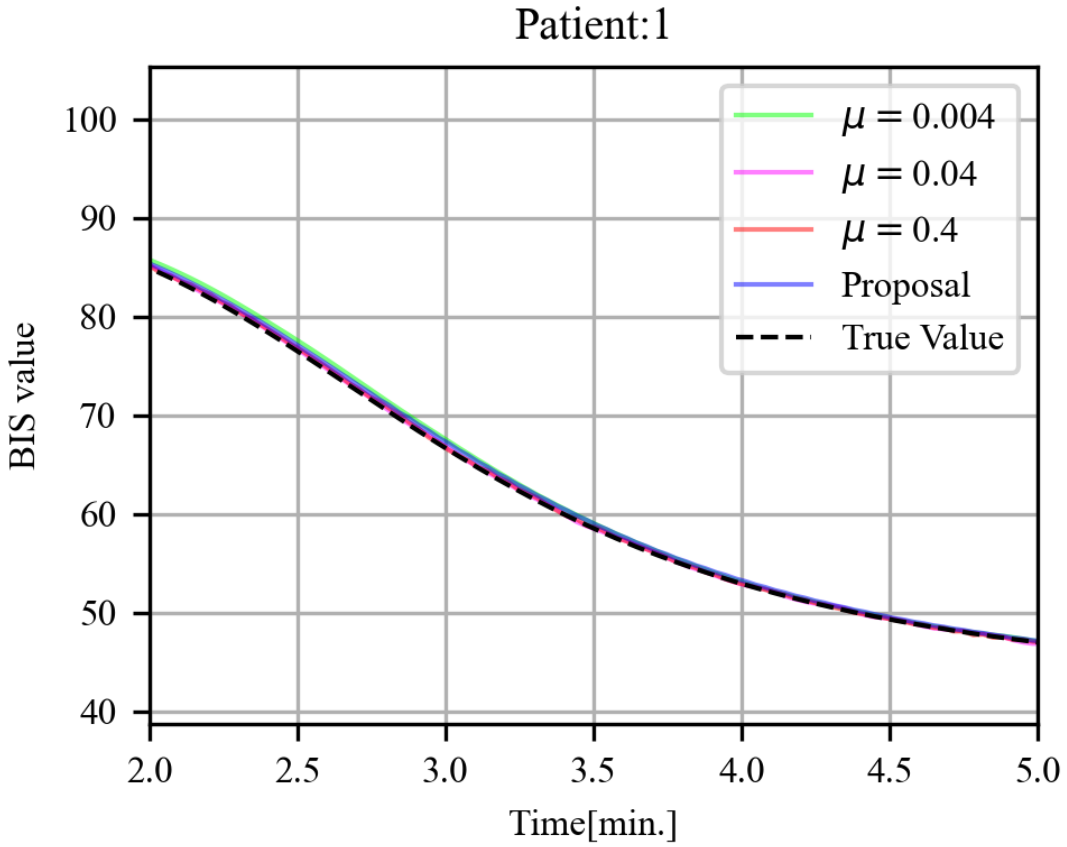

Figure 5.23 Transition of the BIS value in the Patient 1(Compared with Adam,enlarged view)

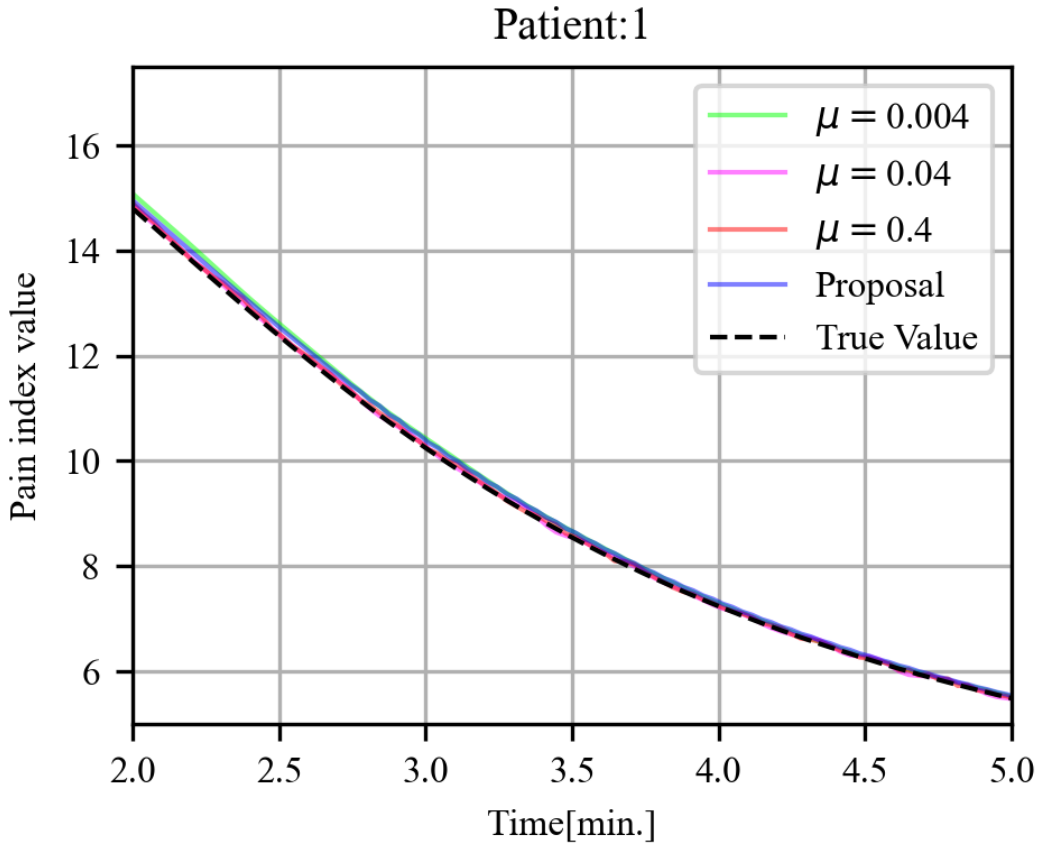

Figure 5.24 Transition of the PI value in the Patient 1(Compared with Adam,enlarged view)

From Fig. 5.23 and 5.24,it can be seemed that the estimated BIS and PI when the parameter μ is fixed at 0.004 converges slowly compared with other cases. Moreover, the estimated BIS and PI when the parameter μ is fixed at 0.04 and 0.4 seem to be closer to the true value compared with those of proposal.

Figure 5.25 and 5.26 shows the squared error between the estimated BIS and PI values by the RNN model and the true value.

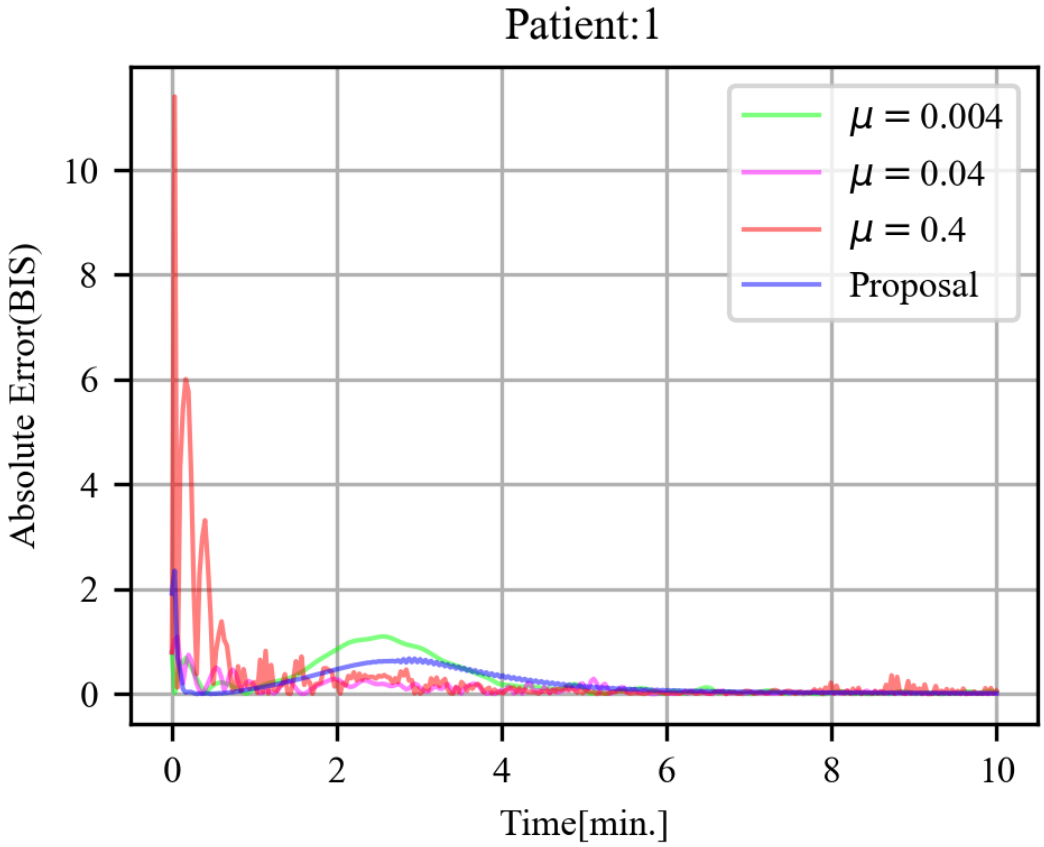

Figure 5.25 Transition of absolute error in the Patient 1(BIS,Compared with Adam)

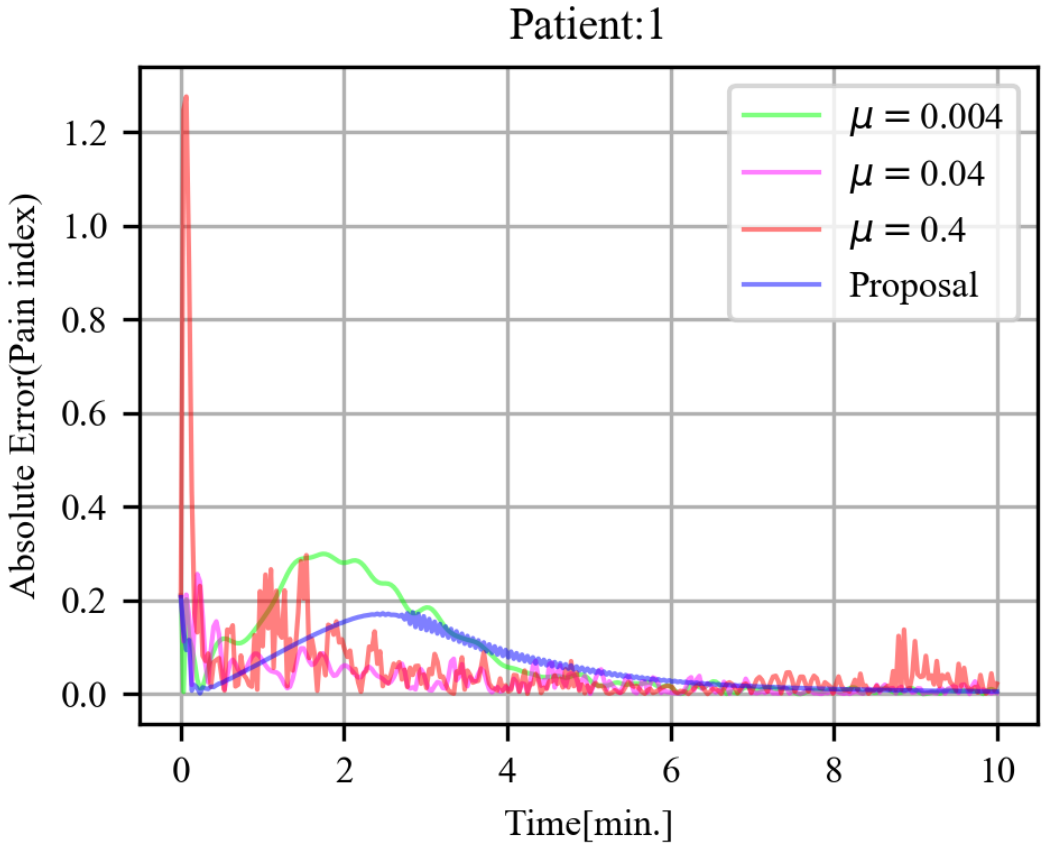

Figure 5.26 Transition of absolute error in the Patient 1(PI,Compared with Adam)

From figure 5.25 and 5.26, it is confirmed that the absolute error in the case the parameter μe are fixed to 0.004 and 0.4 takes higher value compared with the other results. Especially,in the parameter μ is fixed to 0.4, the absolute error takes higher than 10(BIS) and 1.2(PI) around 1 minute.

Next, fig. 5.27 and 5.28 shows enlarged view of fig. 5.25 and 5.26(from 2 to 5 minutes).

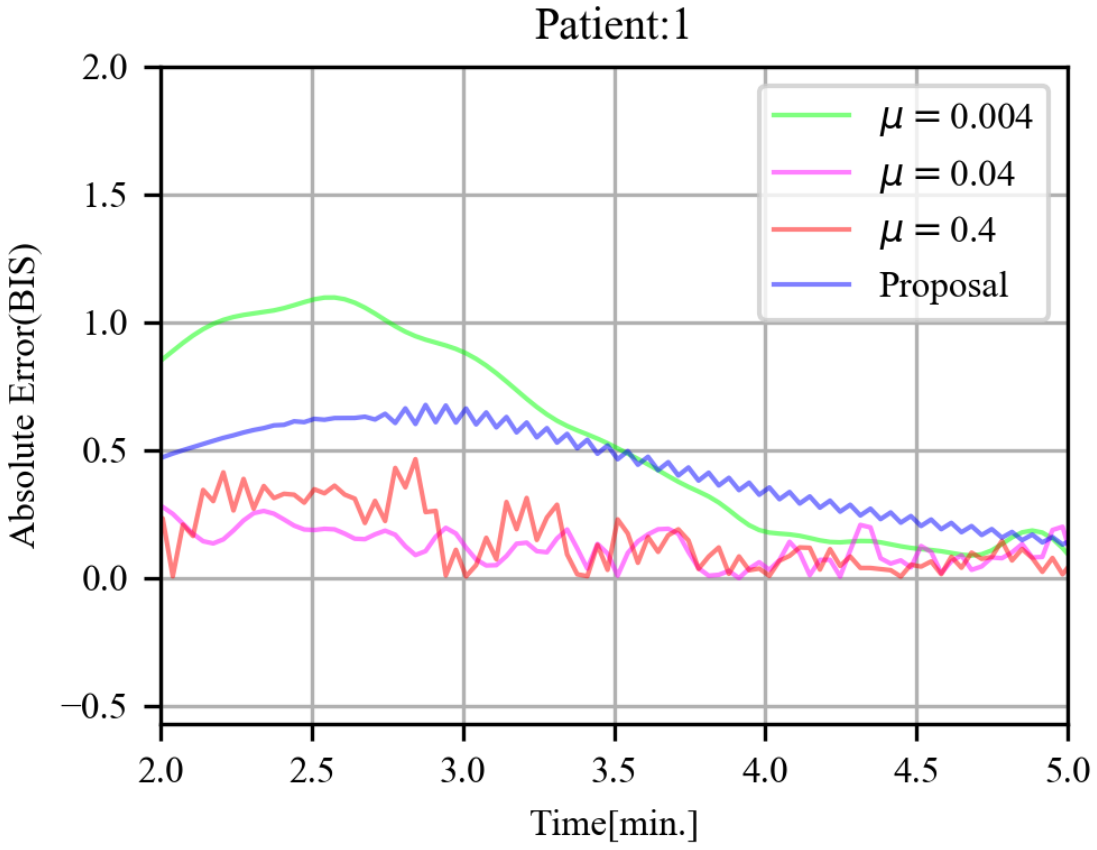

Figure 5.27 Transition of absolute error in the Patient 1(BIS,Compared with Adam,enlarged view)

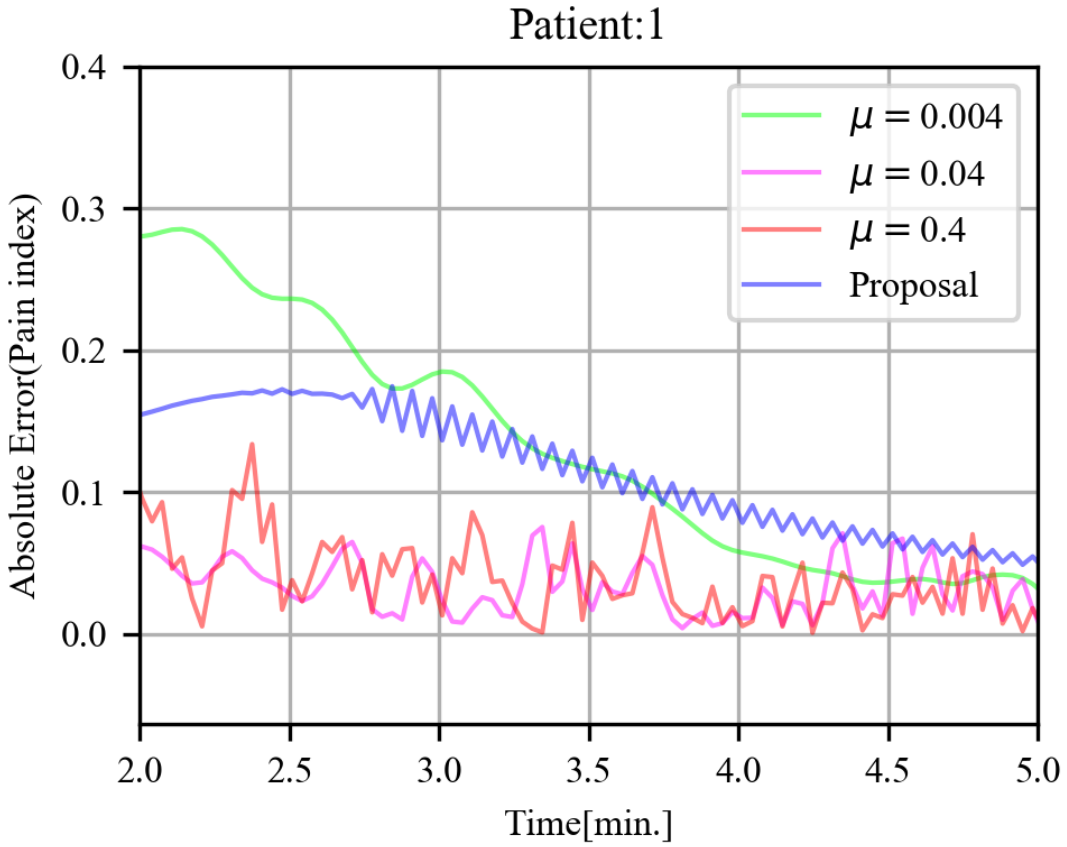

Figure 5.28 Transition of absolute error in the Patient 1(PI,Compared with Adam,enlarged view)

From Fig. 5.27 and 5.28, absolute error in each vital when the parameter μ is fixed at 0.004 takes higher than those of proposal. However, it can also be seen that the absolute error of the proposed method is slightly higher than that of the conventional method when the parameter μ are fixed at 0.04 and 0.4. The reason for such a result is that the proposed method uses a learning rate limited within the range satisfying the stability condition, so that the follow-up speed for a steep change is suppressed.

From those results, it is confirmed that the efficiency and drawbacks of our proposed scheme compared to the scheme with a various parameter μ. In particular, although the advantage of the proposed method is that it does not require tuning of hyper-parameters, it was also found that Adam gives better results depending on Adam's parameter settings. Therefore, it is considered necessary to further improve the proposed method in consideration of the nature

of Adam.

5.4 Summary of the chapter

This section describes the summary of the proposed stable learning scheme. This section proposes the stable learning scheme based on the Lyapnov's stability of the RNN. Using proposed scheme, the RNN can be learned not to oscillate the output compared with the some conventional case in the SGD and RMSprop. Also, it can be confirmed that the output of the RNN can reached faster using proposed scheme compared with the conventional. However, it was confirmed that Adam gave better results than the proposed method depending on parameter tuning of Adam.

As the further study, the drawback of the proposal is need to be analysed. For example, in the proposal, calculation complexity is higher than SGD due to the calculation of adaptive learning rate. Especially, as the total number of weighting coefficients increases, the amount of calculation increases. Therefore, the dimensions and computational complexity of RNNs need to be evaluated. In addition, although the proposed method was devised by modifying SGD, it is also an issue to improve the proposed method considering the moment of gradient like Adam.Furthermore, although the initial value of the weight in the RNN was determined by performing pre-learning this time, it is also necessary to evaluate the performance of the proposed method when pre-learning is not performed. In particular, depending on the initial value, the neural network converges to a local optimum far from the global optimum solution. Therefore, it is necessary to analyze based on the existence of the local optimum and propose a method to get out of the local optimum.

Chapter 6

Pre-processing of the Training Data for the Artifact Detection

6.1 Overview of the pre-processing and artifacts in vital data

This chapter describes the artifact detection method for each vital data. First, in this study, it is assumed that instantaneous artifacts such as ECG R waves as detection targets. (Artifacts that last for a long time are not included.) Also, as a premise, the subject in this proposal is time-series data, and it is considered that it does not change suddenly in adjacent sample times. On the contrary, if it changes suddenly, it is highly likely that it is an artifact.

Based on the above assumptions, this thesis proposes a method to detect artifacts based on the difference information by taking the difference between the previous sample time $t-1$ and the current sample time t.

6.2 Pre-processing algorithm using difference of vital data

Here, the details of the artifact detection method will be described. From the assumptions mentioned in the previous section, it is considered that the values before and after the vital data do not change abruptly. Therefore, if the current data $x[t]$ does not artifact, the difference between the values one step before $\Delta x[t]$ is considered to be close to 0. On the contrary, when the current data $x[t]$ is an artifact, $\Delta x[t]$ is considered to be larger than when it is not an artifact. Based on the above, this thesis proposes an artifact detection method using the difference before and after each data point. Figure 6.1 shows a flowchart of

artifact detection.

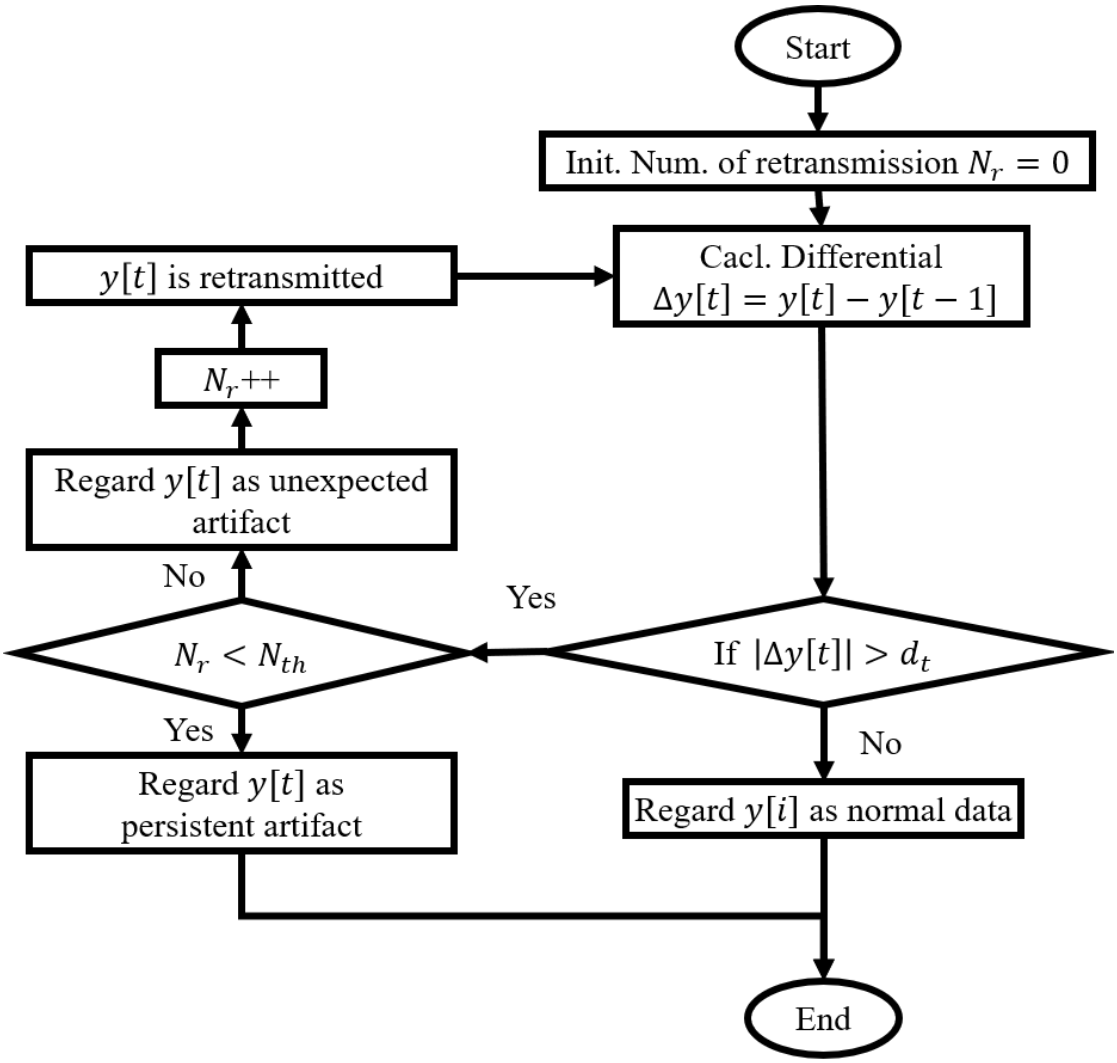

Figure 6.1 Flowchart of the artifact detection algorithm

As shown in Figure 6.1, first calculate the difference $\Delta x[t]$ between the current time data and the data up to one step before. If $\Delta x[t]$ is equal to or greater than the threshold value d_t, $y[t]$ is regarded as an artifact, and if not, it is regarded as a normal value. If even one artifact is detected in the vital data at each time used for learning by this method, the proposed system warns the vital sensor that it may contain artifacts and requests that the vitals be re-transmission as shown in Fig. 4.2.

In this method, there is a false-positive / false-negative trade-off depending on the threshold value for detecting artifact. Specifically, if the threshold value is set low, the probability of detecting an artifact (true positive) increases, but

the probability of treating non-artifact data as an artifact (false positive) also increases. Conversely, if the threshold is set high, false positives will be low, but there is a high possibility that artifacts will be missed. Therefore, in the next section, it is analyzed that theoretically the trade-off between false positives and true positives.

6.3 Theoretical analysis of trade-off between TP/FP

This chapter describes the trade-off between True positive and False positive in the results of artifact detection.

First, non-artifact vital observations are modeled as white Gaussian noise is added to the true value. The observed normal value $y_n[t]$ is as shown in the following equation:

$$y_n[t] = y[t] + n[t]. \tag{6–1}$$

Here, since the probability density function $p_n(x)$ of the amplitude of the noise $n[t]$ is AWGN, it becomes as follows:

$$p_n(x) = \frac{1}{\sqrt{2\pi}\sigma_n} \exp(-\frac{x^2}{2\sigma_n}). \tag{6–2}$$

where, σ_n denotes the standard deviation(SD) of the noise. Next, the vital data with added artifacts will be described. This is also modeled as adding noise $a[t]$ to the true value. In other words, the equation is expressed as follows:

$$y_o[t] = y[t] + a[t]. \tag{6–3}$$

Assuming that the mean amplitude of the artifact is $\bar{a}$ and the probability density function of the amplitude is normally distributed with the variance of the amplitude σ_a, then the probability density function of the amplitude of $a[t]$ can be expressed as follows:

$$p_a(x) = \frac{1}{\sqrt{2\pi}\sigma_a} \exp(-\frac{(x-\bar{a})^2}{2\sigma_a}). \tag{6–4}$$

Here, assuming that the error between the true values of the $y[t]$ and $y[t]$ approximated to be 0, The difference when the vital values of the adjacent step times are both normal values is expressed by the following equation:

$$\begin{aligned} \Delta y[t]_{nn} &= y_n[t] - y_n[t-1] \\ &= (y[t] + n[t]) - (y[t-1] + n[t-1]) \\ &= n[t] - n[t-1]. \end{aligned} \tag{6–5}$$

Since $n[t]$ and $n[t-1]$ are independent and the probability density function is expressed by eq. (6–2), based on the reproductive property of the normal distribution, the probability density function of $\Delta y[t]_n$ is represented by a normal distribution with mean 0 and variance $2\sigma_n^2$:

$$p_{dnn}(x) = \frac{1}{2\sqrt{\pi}\sigma_n} \exp(-\frac{x^2}{4\sigma_n}). \tag{6–6}$$

While, if an artifact is observed in the step time $t-t$ and current step time t is not, the difference between the observed values $\Delta y[t]_{an}$ a is expressed by the following equation:

$$\begin{aligned} \Delta y[t]_{an} &= y_n[t] - y_n[t-1] \\ &= (y[t] + n[t]) - (y[t-1] + a[t-1]) \\ &= n[t] - a[t-1]. \end{aligned} \tag{6–7}$$

Here, $n[t]$ and $a[t-1]$ are independent of each other, and $a[t-1]$ is expressed by the probability density function of eq. (6–4) and $n[t]$ is expressed by the probability density function of eq. (6–2). Therefore, from the reproductive property of the normal distribution, the probability density function of $\Delta y[t]_{an}$ ($p_{dan}(x)$) is represented by the normal distribution with mean $-\bar{a}$and variance $\sigma_n^2 + \sigma_a^2$:

$$p_{dan}(x) = \frac{1}{2\sqrt{\pi(\sigma_n^2 + \sigma_a^2)}} \exp[-\frac{(x+\bar{a})^2}{2(\sigma_n^2 + \sigma_a^2)}]. \tag{6–8}$$

In other words, the probability density function when the value of the current step is a normal value is expressed by a gaussian mixture model of equations (6–6) and (6–8):

$$\begin{aligned} p_{da}(x) &= \alpha p_{dnn} + (1-\alpha) p_{dan} \\ &= \frac{\alpha}{2\sqrt{\pi}\sigma_n} \exp(-\frac{x^2}{4\sigma_n}) + \frac{1-\alpha}{2\sqrt{\pi(\sigma_n^2 + \sigma_a^2)}} \exp[-\frac{(x+\bar{a})^2}{2(\sigma_n^2 + \sigma_a^2)}], \end{aligned} \tag{6–9}$$

where, α denotes the abundance ratio of normal values in the data. Also, the cumulative distribution function of the normal distribution with mean $\bar{x}$ variance σ^2 can be expressed as follows:

$$\begin{aligned} P(x) &= \int_{-\infty}^{x} \frac{1}{2\sqrt{\pi\sigma^2}} \exp[-\frac{(a-\bar{x})^2}{2\sigma^2}] da \\ &= \frac{1}{2} erfc(-\frac{x-\bar{x}}{\sqrt{2}\sigma_a}), \end{aligned} \tag{6–10}$$

where, $erfc(x)$ is called the complementary error function and is defined by the following equation:

$$erfc(x) = \frac{2}{\sqrt{\pi}} \int_x^\infty \exp(-t^2)dt. \tag{6–11}$$

Therefore, considering that it is determined to be an artifact when the difference $\Delta y[t]$ is equal to or greater than the threshold value d_t, the probability that a normal value is determined to be an artifact from the equation (false positive probability) $P_{FPR}(x)$ is as follows:

$$\begin{aligned} P_{FPR}(x) &= \int_{d_t}^\infty p_{dn}(x)dx \\ &= \int_{d_t}^\infty \frac{\alpha}{2\sqrt{\pi}\sigma_n} \exp(-\frac{x^2}{4\sigma_n}) + \frac{1-\alpha}{2\sqrt{\pi(\sigma_n^2+\sigma_a^2)}} \exp[-\frac{(x+\bar{a})^2}{2(\sigma_n^2+\sigma_a^2)}]dx \\ &= \alpha[1 - \frac{1}{2}erfc(-\frac{x}{2\sigma_n})] + (1-\alpha)\{1 - \frac{1}{2}erfc[-\frac{x+\bar{a}}{\sqrt{2(\sigma_n^2+\sigma_a^2)}}]\} \\ &= 1 - \frac{\alpha}{2}erfc(-\frac{x}{2\sigma_n}) - \frac{1-\alpha}{2}erfc[-\frac{x+\bar{a}}{\sqrt{2(\sigma_n^2+\sigma_a^2)}}]. \end{aligned} \tag{6–12}$$

While, if an artifact is observed in the step time t and previous step time $t-1$ is not, the difference between the observed values $\Delta y[t]_{na}$ a is expressed by the following equation:

$$\begin{aligned} \Delta y[t]_{na} &= y_n[t] - y_n[t-1] \\ &= (y[t] + a[t]) - (y[t-1] + n[t-1]) \\ &= a[t] - n[t-1]. \end{aligned} \tag{6–13}$$

Here, $a[t]$ and $n[t-1]$ are independent of each other, and $a[t]$ is expressed by the probability density function of eq. (6–4) and $n[t]$ is expressed by the probability density function of eq. (6–2). Therefore, from the reproductive property of the normal distribution, the probability density function of $\Delta y[t]_a$ ($p_{da}(x)$) is represented by the normal distribution with mean $\bar{a}$and variance $\sigma_n^2 + \sigma_a^2$:

$$p_{da}(x) = \frac{1}{2\sqrt{\pi(\sigma_n^2+\sigma_a^2)}} \exp[-\frac{(x-\bar{a})^2}{2(\sigma_n^2+\sigma_a^2)}]. \tag{6–14}$$

Therefore, from eq. (6–14), the probability that an artifact can be detected

correctly(True Positive Rate: $P_{TPR}(x)$) can be expressed as follows:

$$\begin{aligned} P_{TPR}(x) &= \int_{d_t}^{\infty} p_{da}(x)dx \\ &= \int_{d_t}^{\infty} \frac{1}{2\sqrt{\pi(\sigma_n^2+\sigma_a^2)}} \exp[-\frac{(x-\bar{a})^2}{2(\sigma_n^2+\sigma_a^2)}]dx \\ &= 1 - \frac{1}{2} erfc(-\frac{x-\bar{a}}{\sqrt{2(\sigma_n^2+\sigma_a^2)}}). \end{aligned} \tag{6–15}$$

Using the TPR/FPR theoretical formulas shown in equations (6–12) and (6–15), the next section compares the TPR/FPR obtained from the simulation results with the theoretical formulas and evaluates a trade-off relationship.

6.4 Performance evaluation

6.4.1 Simulation conditions

In this section, some evaluations to confirm the prediction accuracy of our proposal are performed. Here, assuming the administration of anesthesia to the patient during surgery, the estimation performance of vitals corresponding to each of the administration of a sedative and an analgesic is evaluated using same vital as Chap. 5.

Thus, the BIS and PI behaviors of 12 patients are simulated to evaluate the efficiency of our proposal. Model used in simulation is the same as Chap. 5 and parameter of the patient is shown in table 5.1.

The Dosages in each time step were controlled by the same way of Chap. 5. Furthermore, to evaluate the efficiency of the threshold used in the artifact detection, four type of threshold are given in the simulation.

Table 6.1 shows the simulation parameters.

Table 6.1 simulation parameters

simulation time[min.]	20
Sampling Period T_s[sec.]	2.0
Gain of the PID controller	
Proportional Gain: K_p	0.055
Integral Gain: K_i	0.001
Derivative Gain: K_i	2.68
Target BIS value in the control	50.0
Target PI value in the control	4.5
Learning method	Proposed in Chap. 5
Number of units in hidden layer N	
(the size of weight vectors)	10
Activation function in hidden layer	Sigmoid
Activation function in output layer	Linear
Number of hidden layers	1
Signal to Noise Ratio(SNR) [dB]	20
Artifact adding interval [sec.]	30
Artifact parameters	
Relative average amplitude	0.56
Relative standard deviation of amplitude	0.10
Relative average amplitude of noise(to normal data)	0.10
Threshold of the proposed scheme	0.14,0.28,0.42,0.56

In this simulation, the detection rate and false detection rate of artifacts and their influence on vital estimation are evaluated. To simulate the noise in real vital data, White Gaussian Noise are added in observed vital. The relative average amplitude of noise shown in the table 6.1 is a relative value supposing that the average amplitude of standardised vitals is 1. Moreover, to simulate artifact(e.g. ECG R-wave), artifacts are added to the true value every 30 seconds. The probably density function of the artifact is shown in eq. (6–4) and parameters are shown in table 6.1. Notice that, this decibel notation is a relative value when the average amplitude of standardised BIS value is 1. Finally, in the simulation, threshold of the artifact detection is changed. In the simulation, threshold are decided to became integer multiple of the $\sqrt{2}\sigma_n$. The value $\sigma_{dn} = \sqrt{2}\sigma_n$ denotes the SD of the difference $\Delta y[t]_n$.

6.4.2 Numerical results

Here, the simulation results is described. The MAE of this period is shown in Figure 6.2.

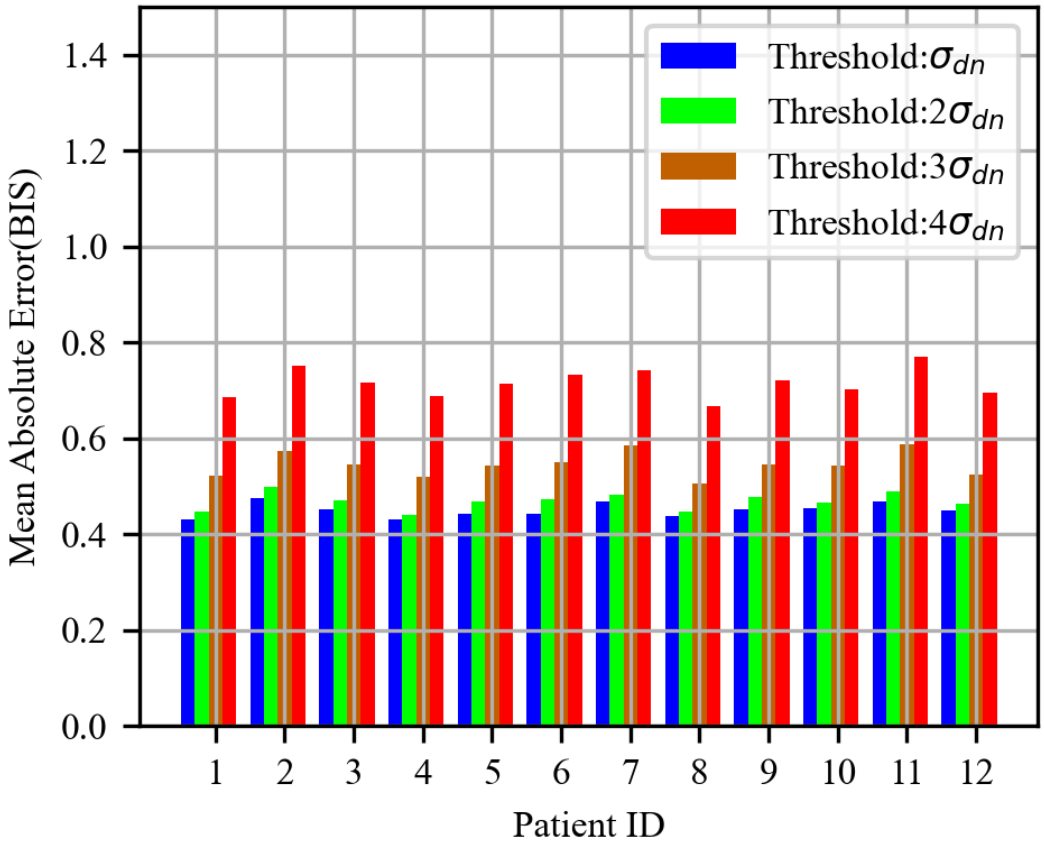

Figure 6.2 Mean Absolute Error in each patient(BIS with artifact)

From figure 6.2, it can be confirmed that the higher the threshold value, the higher the MAE value. It is considered that this is because if the threshold value is too high, the number of undetected artifact increases.

Next, the performance evaluation for each patient will be described. Figure 6.3 and shows the transition of the BIS value of the Patient 1.

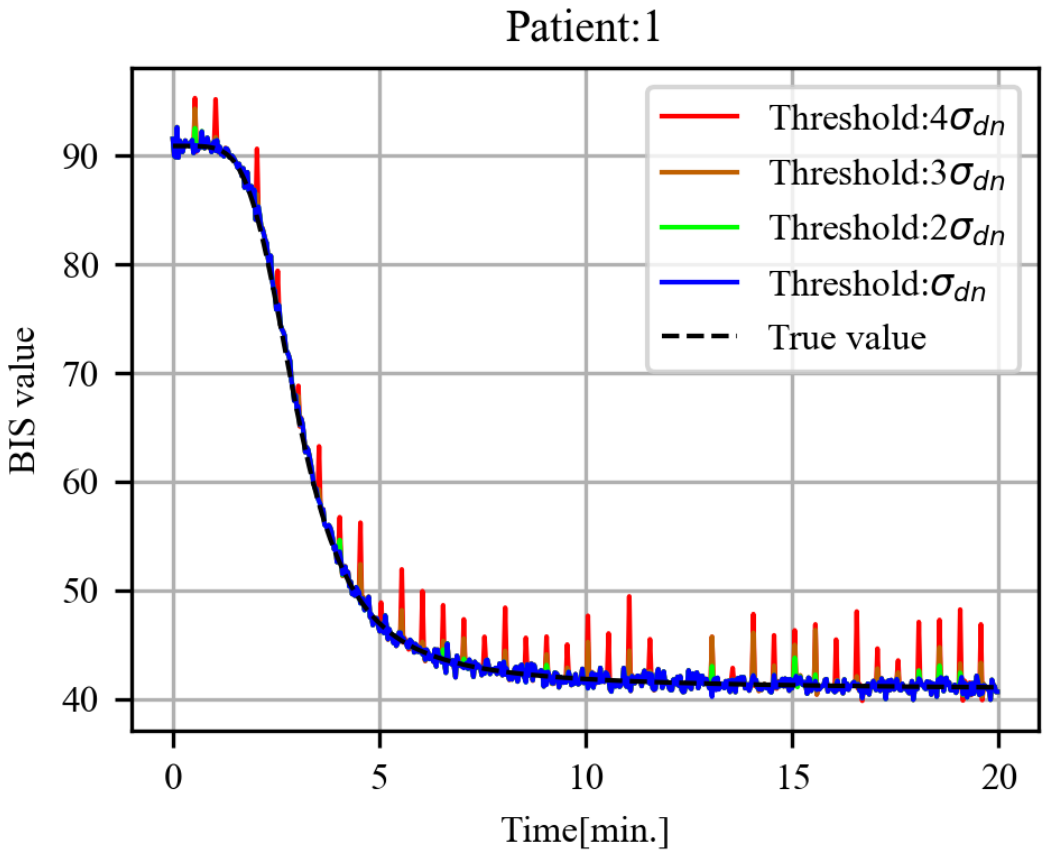

Figure 6.3 Transition of the BIS value in the Patient 1(with artifact)

From Fig. 6.3, the estimated BIS value in the case that threshold is σ_{dn} seems to take closer to true value compared with other case. Also, it can be confirmed that estimated BIS in the case threshold are $3\sigma_{dn}$ and $4\sigma_{dn}$ sometime deviates from the true value at the timing when the artifact occurs. This may be because the threshold is too high to detect the artifact.

Figure 6.4 shows the squared error between the estimated BIS and PI values by the RNN model and the true value.

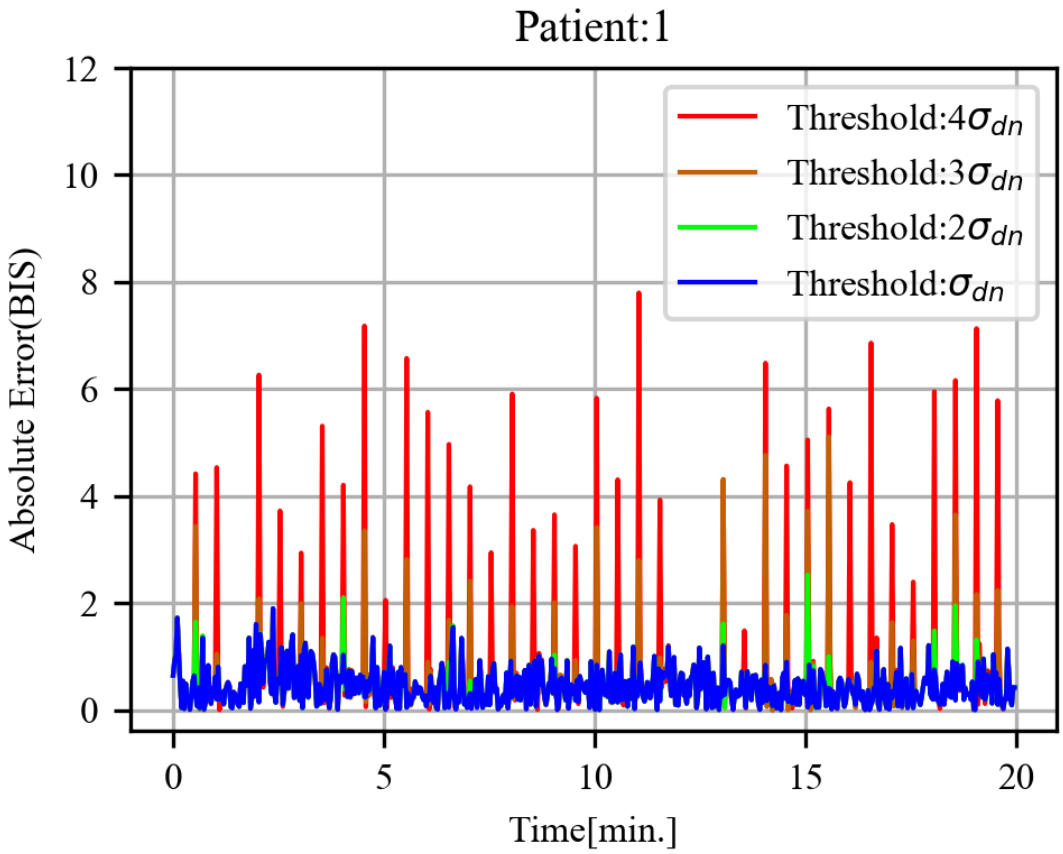

Figure 6.4 Transition of squared error in the Patient 1(BIS,with artifact)

From figure 6.4 and, it is confirmed that the absolute error in the case threshold are $3\sigma_{dn}$ and $4\sigma_{dn}$ (i.e., the blue line) takes higher value.

From these results, it can be confirmed that many undetected cases occur depending on the threshold value of artifact detection.

Next, relationships between True/False Positive and True/False Negative is evaluated. Figure 6.5 ,6.6, 6.7 and 6.8 show the distribution of differences in vital values (standardized) and the judgment results of all patients during simulation for each threshold.

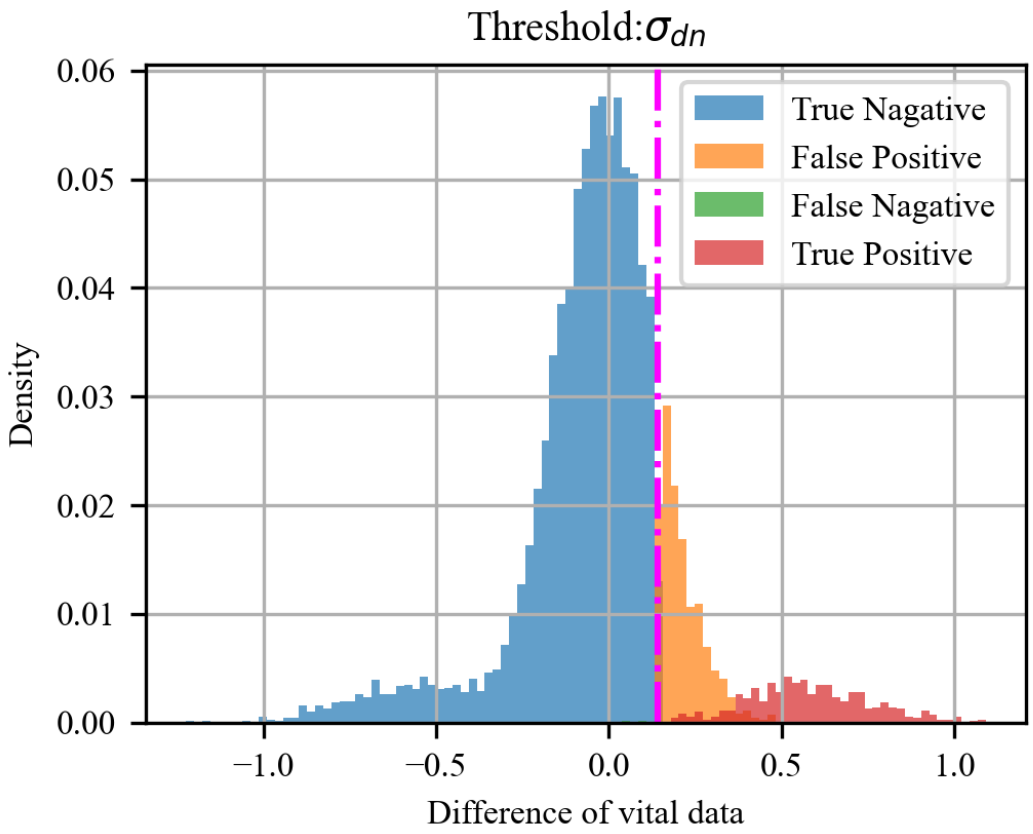

Figure 6.5 Distribution of judgment results(Threshold:σ_{dn})

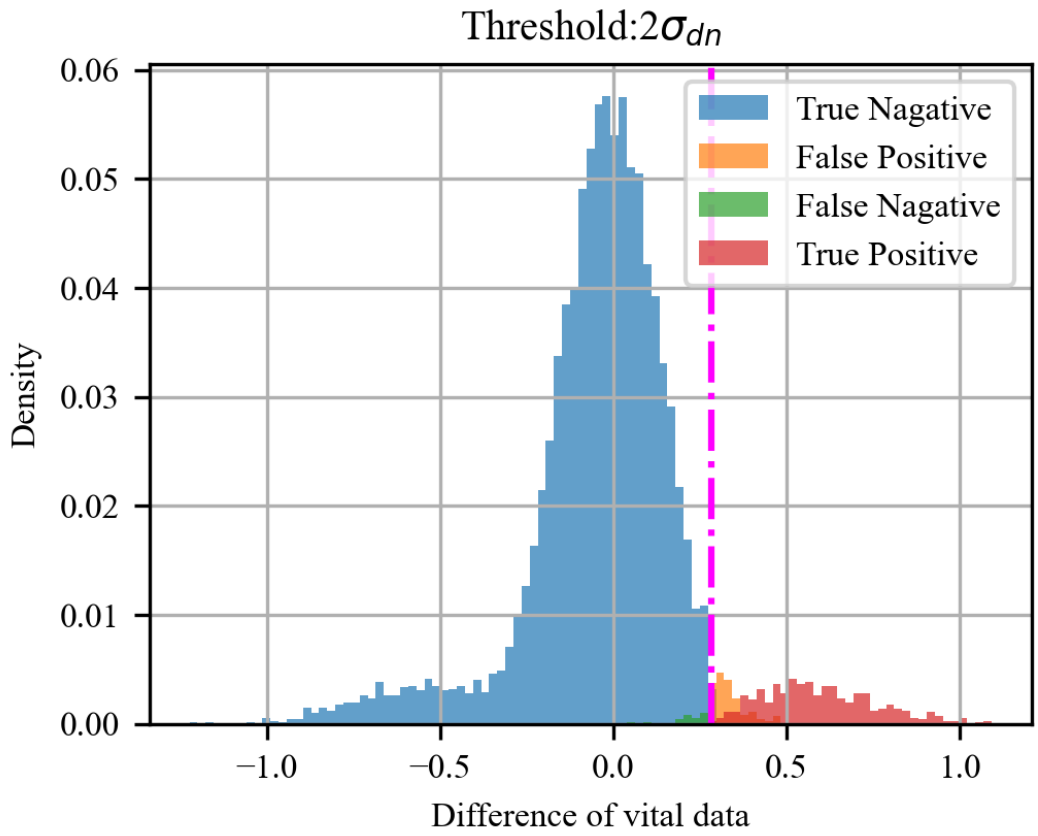

Figure 6.6 Distribution of judgment results(Threshold:2σ_{dn})

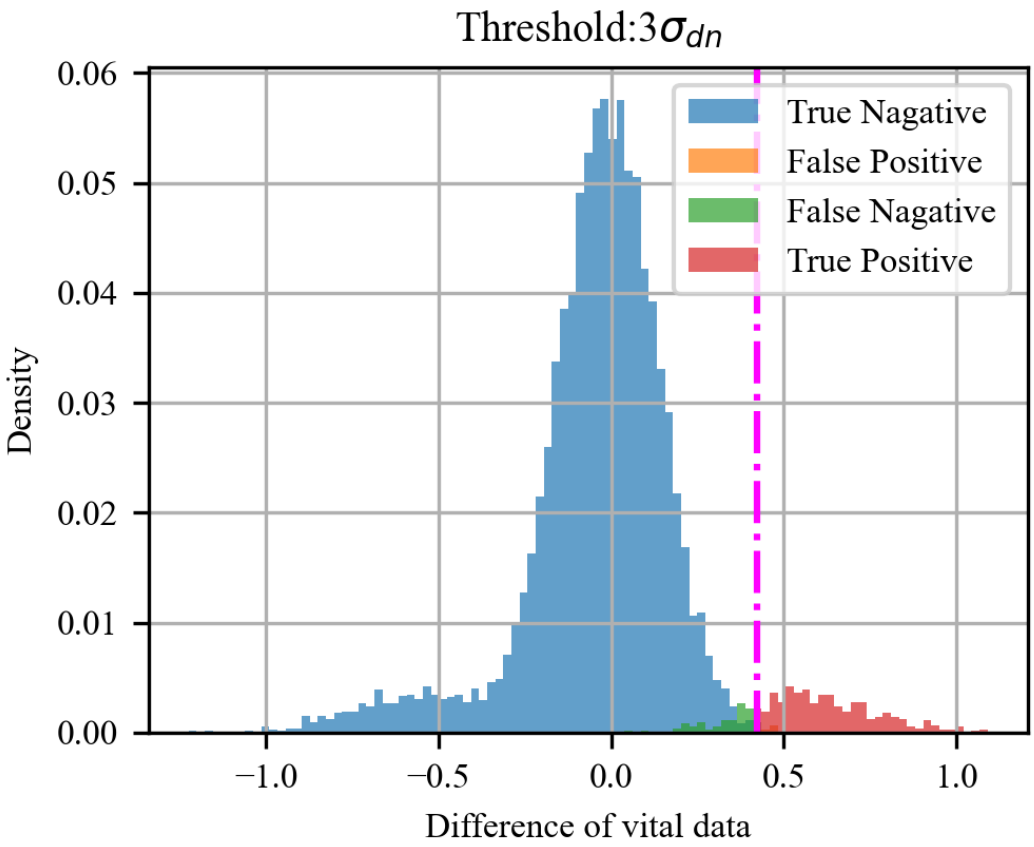

Figure 6.7 Distribution of judgment results(Threshold:3σ_{dn})

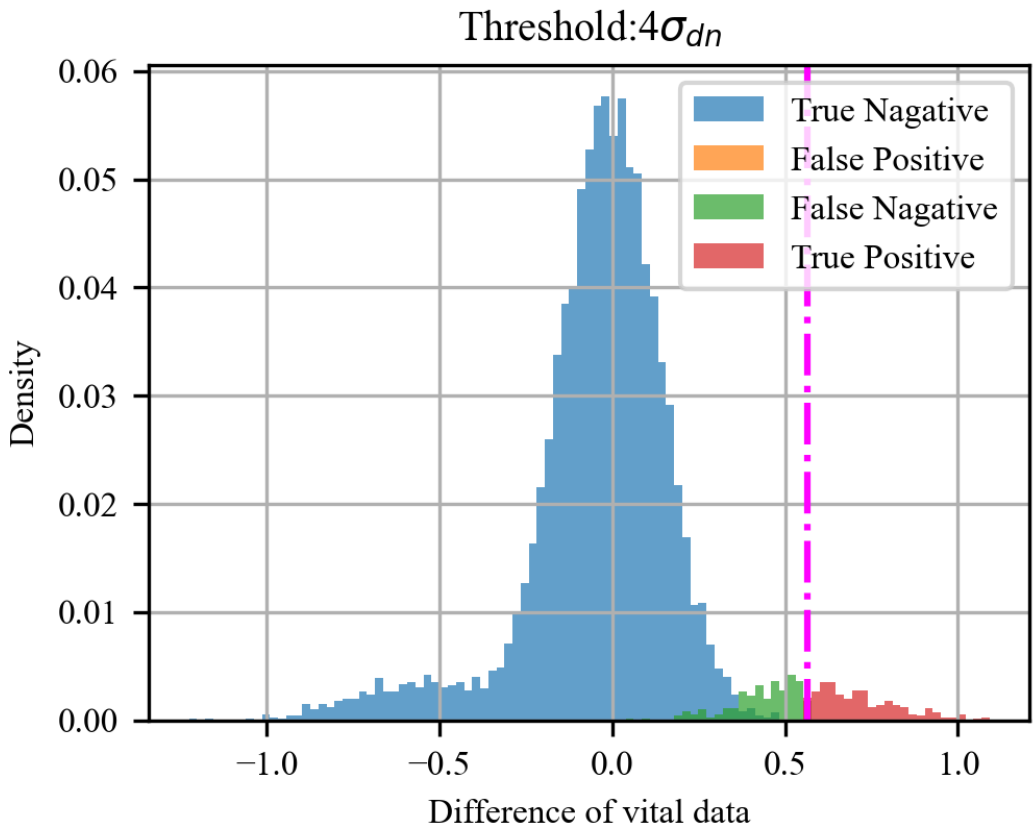

Figure 6.8 Distribution of judgment results(Threshold:4σ_{dn})

From fig. 6.5 ,6.6, 6.7 and 6.8,it can be seen that the higher the threshold, the greater the number of undetected artifacts(False Negative). While, it can also be seen that the lower the threshold value, the greater the number of erroneous defections of normal values(False Positive). In this proposed system, the more false positives, the more times the determiner warns the system. Therefore, it can be said that the threshold value for artifact detection needs to be determined in consideration of the trade-off between false detection and non-detection.

Finally, the theoretical value of the ROC curve and the simulation result are compared in order to evaluate the trade-off relationship between TPR and FPR. The theoretical value of ROC curve is calculated using eqs. (6–12) and (6–15). Figure 6.9 shows the ROC curve and TPR and FPR evaluated in the simulation.

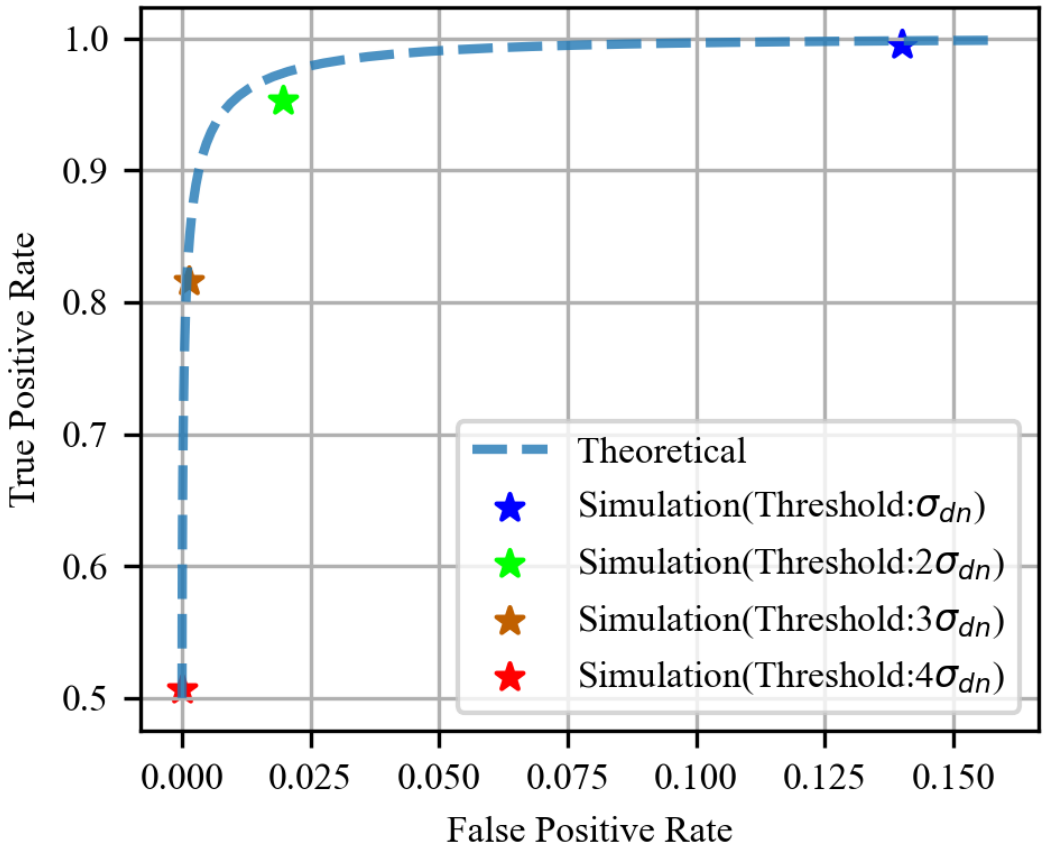

Figure 6.9 ROC curve

From the figure, it can be seen that the TPR / FPR calculated from the simulation results generally agrees with the theoretical values derived in previous sections. For each simulation value, the false positive rate is almost 0 in the result when the threshold value is $4\sigma_{dn}$. However, since the detection rate is about 0.5, it can be seen that about half of the artifacts cannot be detected. While, when the threshold value is 1, the TPR is close to σ_{dn}. However, the false positive rate is also around 0.15. This means that an artifact detection warning is issued to the system once every 10 samples on average, and it can be said that the load on the system due to the warning is higher than in the case of other threshold values. Regarding the results when other threshold values are used, it can be said that when the threshold value is $2\sigma_{dn}$, the value is closest to the cutoff point (FPR = 0, TPR = 1) of the ROC curve and is close to the equilibrium point of the trade-off. Finally, looking at the results at threshold $3\sigma_{dn}$, it seems that they are farther from the cutoff point than at threshold $2\sigma_{dn}$, and the TPR is

about 0.15 lower.

6.5 Summary of the chapter

This section describes the summary of the proposed stable learning scheme. This section proposes the artifact detection method using difference of the data. Also, theoretical analysis of trade-off between TPR/FPR in the detecting artifacts using proposed scheme is performed. Numerical evaluation shows the effect of artifact in the learning of RNN. Furthermore, the trade-off of TPR / FPR due to the threshold of artifact detection and its effect on the system were also considered.

Future issues include not only the instantaneous artifacts assumed this chapter, but also countermeasures when continuous artifacts are mixed in the learning data. In particular, it seems to be sufficient to determine whether the data that appear to be continuous artifacts are true artifacts or due to abrupt changes in pharmacokinetics and pharmacodynamics of the patient. In addition, considering the practicality, it is also an issue to propose a method of learning the probability distribution of the amplitude of the artifact and determining the artifact detection threshold based on the learning result.

Chapter 7

Conclusion and future works

7.1 Conclusion

This thesis proposes a dependable learning scheme for the prediction model of the drug effect using RNN. RNNs are effective in identifying non-linear and non-stationary systems. However, in order to perform more reliable learning, it is necessary to consider the characteristics of vitals used for parameter tuning and learning. Based on the above, this thesis made two proposals in order to make the prediction of drug effect by RNN more dependable.

First, when predicting the medication effect with RNN, the stability of the output of RNN is important. From the point of view, this thesis proposed a method that can learn at high speed without making the output of the neural network unstable during learning. In particular, the stability of the RNN model is analysed using Lyapunov analysis and the optimum learning rate for each parameter of the RNN model is derived. The prediction performance of our proposed scheme against a conventional learning method is evaluated by the numerical simulation.

It is also proposed that an artifact detection method using the difference in vital data in order to improve the robustness against artifacts derived from the electrocardiogram mixed in vitals. It also evaluated that the trade-off between TPR and FPR (TNR and FNR) of artifacts due to the threshold value in artifact detection in the proposed method.

7.2 Future works

In the future research, It is necessary to study a method for predicting and controlling the medication effect using the proposed system. For that purpose,

the effective control scheme of drug effect using the RNN model learned with our proposed scheme should be considered. Furthermore, it is necessary to consider a method for detecting not only the instantaneous artifacts assumed this time but also continuous artifacts. In addition, the proposed scheme should be implemented for using similar applications. For example, the application to predict risk of the car accident and autonomous car control should be considered.

付録 A

Numerical model of anesthetic effect

This section describes numerical model of the drug effects which is applied in numerical evaluation.

A.0.1 Compartmental model

In this study, it is applied that the fourth-order compartmental model proposed by Schnider and Minto [19] as the Pharmacokinetic (PK) and Pharmacodynamics (PD) model for Propofol (Sedative) and Remifentanil (Analgesics). The compartmental model is shown in Fig. A.1 and expressed as

$$\begin{aligned}
&\dot{C}_1(t) = -(k_{1o} + k_{12} + k_{13}) \cdot C_1(t) + k_{21} \cdot C_2(t) \\
&+k_{31} \cdot C_3(t) + \frac{\dot{u}(t)}{V_1} \\
&\dot{C}_2(t) = k_{12} \cdot C_1(t) - k_{21} \cdot C_2(t) \\
&\dot{C}_3(t) = k_{13} \cdot C_1(t) - k_{31} \cdot C_3(t) \\
&\dot{C}_e(t) = -k_e \cdot C_e(t) + k_e \cdot C_1(t).
\end{aligned} \tag{A–1}$$

where, C_i represents the concentration in the compartment i and C_e denotes the concentration in the effect site compartment[mg/L], k_{ij} ($i \neq j$) is the drug absorption frequency from compartment i to j, k_{1o} is the drug metabolize frequency from compartment 1 and k_e is the drug absorption frequency from compartment 1 to effect site compartment and the frequency of drug removal from effect site compartment, The parameter $\dot{u}$ represents the drug infusion rate [mg/s], and V_i is the volume of the compartment i respectively. In the Model [19], it is assumed that the effect site compartment is included in the compartment1. Consequently, the drug concentration of the compartment 1 is not decreased by the drug absorption to the effect site compartment.

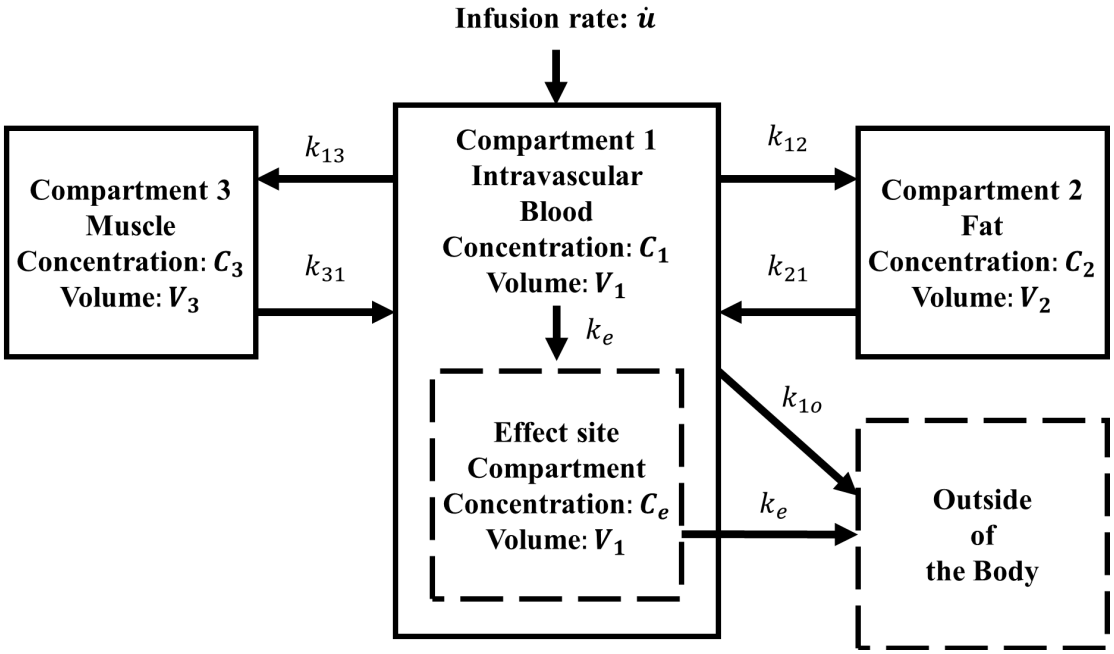

Figure A.1 PK-PD model

Each rate constant and volume of each compartment are modeled by age, weight, height and gender .In the hypnotic drug case, each parameter are defined as follows[19]:

$$
\begin{aligned}
&k_{1o} = \frac{Cl_1}{V_1}[\mathrm{s}^{-1}], \mathrm{k}_{12} = \frac{\mathrm{Cl}_2}{\mathrm{V}_1}[\mathrm{s}^{-1}], \mathrm{k}_{13} = \frac{\mathrm{Cl}_3}{\mathrm{V}_1}[\mathrm{s}^{-1}] \\
&k_{21} = \frac{Cl_2}{V_2}[\mathrm{s}^{-1}], \mathrm{k}_{31} = \frac{\mathrm{Cl}_3}{\mathrm{V}_3}[\mathrm{s}^{-1}], \mathrm{k}_{\mathrm{e}} = 0.0076[\mathrm{s}^{-1}] \\
&V_1 = 4.27[\mathrm{L}], \mathrm{V}_2 = 18.9 - 0.391 \cdot (\mathrm{a} - 53)[\mathrm{L}] \\
&V_3 = 2.38[\mathrm{L}] \\
&Cl_1 = [1.89 + 0.456(w - 77) - 0.0681(lbm - 59) \\
&+0.264(h - 177)]/60[\mathrm{L/s}] \\
&Cl_2 = [1.29 + 0.024(1 - 53)/60[\mathrm{L/s}] \\
&Cl_3 = 0.0139[\mathrm{L/s}],
\end{aligned}
\tag{A–2}
$$

where, Cl_i is the rate at which the drug is removed from compartment i and parameters a,h and w denotes age, height[cm] and weights[kg] of the patients respectively. Also, the parameter lbm means lean body mass and the parameter is defined as follows:

$$
lbm = \begin{cases} 1.1 \cdot w - 128\frac{w^2}{h^2} & (male) \\ 1.07 \cdot w - 148\frac{w^2}{h^2} & (female) \end{cases}. \tag{A–3}
$$

Similarly, parameters for analgesics are defined as follows[2]:

$$
\begin{aligned}
&k_{1o} = \frac{Cl_1}{V_1}[\mathrm{s}^{-1}], \mathrm{k}_{12} = \frac{\mathrm{Cl}_2}{\mathrm{V}_1}[\mathrm{s}^{-1}], \mathrm{k}_{13} = \frac{\mathrm{Cl}_3}{\mathrm{V}_1}[\mathrm{s}^{-1}] \\
&k_{21} = \frac{Cl_2}{V_2}[\mathrm{s}^{-1}], \mathrm{k}_{31} = \frac{\mathrm{Cl}_3}{\mathrm{V}_3}[\mathrm{s}^{-1}], \mathrm{k_e} = 0.595 - 0.007(\mathrm{a} - 40)[\mathrm{s}^{-1}] \\
&V_1 = 5.1 - 0.0201(a - 40) + 0.072(lbm - 55)[\mathrm{L}], \\
&V_2 = 9.82 - 0.0811(a - 40) + 0.108(lbm - 55)[\mathrm{L}] \\
&V_3 = 5.42[\mathrm{L}] \\
&Cl_1 = [2.6 - 0.0162(a - 40) + 0.0191(lbm - 55)]/60[\mathrm{L/s}] \\
&Cl_2 = [2.05 + 0.0301(a - 40)/60[\mathrm{L/s}] \\
&Cl_3 = [0.076 - 0.00113(a - 40)]/60[\mathrm{L/s}].
\end{aligned} \tag{A–4}
$$

A.0.2 Hill equation and response surface model

The BIS value is related to the effect site concentration. The empirical static relationship is typically expressed by the nonlinear function: Hill equation [20]

$$BIS(t) = f_b(C_e(t)) = E_0(1 - \frac{C_e(t)^\gamma}{C_e(t)^\gamma + EC_{50}^\gamma}) \tag{A–5}$$

where, E_0 denotes the value of BIS when effect site concentration C_e is zero, EC_{50} denotes concentration of effect site compartment when value of BIS is $E_0/2$,and γ denotes steepness of BIS variation depending on change of effect site concentration C_e respectively.

Similarly, the pain index(PI)[3] may be related to the concentration of the effect side. In addition, sedatives and analgesics interact with each other for BIS and PI values. Considering those phenomenon, in the paper [3], a response model that extends Hill's equation is constructed:

$$BIS(t) = E_0 - E_{max}[\frac{(C_{e,p} + \phi C_{e,p}C_{e,r})^\gamma}{(C_{e,p} + \phi C_{e,p}C_{e,r})^\gamma + C_{50}^\gamma}], \tag{A–6}$$

$$PI(t) = E_0 - E_{max}[\frac{(C_{e,r} + \phi C_{e,p}C_{e,r})^\gamma}{(C_{e,r} + \phi C_{e,p}C_{e,r})^\gamma + C_{50}^\gamma}], \tag{A–7}$$

where, $C_{e,p}$ and $C_{e,r}$ denotes effect site concentration of sedative(propofol) and analgesic(remifentanil) drug. average parameter of each coefficients in e.q. (A–6) and (A–7) are shown in table A.1.

Table A.1 Average value of response surface model[3]

Parameter	For BIS	For PI
E_0	90.9	19.7
E_{max}	50.4	19.5
C_{50}	2.86	3.01
γ	2.5	1.27
ϕ	2.28	2.53

In this paper, above average values are applied to simulate BIS and PI value.

Published Papers

Reviewed Journal Papers

(1) Yoshitomo Sakuma, Kento Takabayashi, Takumi Kobayashi, Chika Sugimoto and Ryuji Kohno ”Learning Scheme Based on Stability Analysis for Prediction Model of Anesthetic Effect Using Recurrent Neural Network” Published in International Journal of Trend in Research and Development (IJTRD), ISSN: 2394-9333, Volume-7 — Issue-2 , April 2020.

(2) Yoshitomo Sakuma, Kento Takabayashi, Takumi Kobayashi, Chika Sugimoto and Ryuji Kohno ”Dependable Learning Scheme for Prediction Model of Hypnotic and Analgesic effect Using Recurrent Neural Networks” IEEE Access (to be submitted)

International Conference Papers

(1) Yoshitomo Sakuma, Keiko Sameshima and Ryuji Kohno, ”An adaptive scheme of controlling dosage and dosing interval in general anesthesia by model predictive control using anesthetic depth model,” 2017 11th International Symposium on Medical Information and Communication Technology (ISMICT), Lisbon, 2017, pp. 77-81.

(2) Yoshitomo Sakuma and Ryuji Kohno, ”A Dynamic Model Estimation Scheme for Model Predictive Control of Anesthesia Using Recurrent Neural Network,” 2018 12th International Symposium on Medical Information and Communication Technology (ISMICT), Sydney, NSW, 2018, pp. 1-5.

[Best Paper Award]

(3) Yukihiro Kinjo, Yoshiomo Sakuma, Ryuji Kohno, “Laerning and Recognition with Neural Network of Heart Beats Sensed by WBAN for Patient Stress Estimate for Rehabilitation,” The13th EAI International Conference on Body Area Networks 2018 (BODYNETS2018), Oulu, Finland (2018-10), pp. 195-201

(4) Yukihiro Kinjo, Yoshitomo Sakuma, Takumi Kobayashi, Chika Sugimoto and Ryuji Kohno, "Patient Stress Estimation for Using Deep Learning with RRI Data Sensed by WBAN," 2019 13th International Symposium on Medical Information and Communication Technology (ISMICT), Oslo, Norway, 2019, pp. 1-5.

(5) Yoshitomo Sakuma, Takumi Kobayashi, Chika Sugimoto and Ryuji Kohno, "A Fine-Tuning Method Using Pruning of Recurrent Neural Network for Prediction of the Anesthetic Effects," 2020 14th International Symposium on Medical Information Communication Technology (ISMICT), Nara, Japan, 2020, pp. 1-5.

Domestic Conference Papers

(1) Yoshitomo Sakuma, Keiko Sameshima, and Ryuji Kohno, "An Adaptive Scheme Of Controlling Dosage In Surgery Operation By Feedback Control Using Anesthetic Depth Model," IEICE Technical Conference of Healthcare and Medical Information Technology(MICT), pp.35-40, May. 2016. (in Japanese)

(2) Yoshitomo Sakuma, and Ryuji Kohno, "A Study about Remote Control of Dosing Anesthetic Using Model Predictive Control Considering Sparsity of the Control Variables," The 38th Symposium on Information Theory and Its Applications (SITA2017),November 2017. (in Japanese)

(3) Yoshitomo Sakuma, Takumi Kobayashi, Chika Sugimoto and Ryuji Kohno, "Consideration about Learning Scheme with Outlier Detection in Training Data for Prediction Model of Medication Effect Using Recurrent Neural Networks," IEICE Technical Conference of Healthcare and Medical Information Technology(MICT), pp.28-33, January. 2021. (in Japanese)

IEICE Annual Conference Letters

(1) Yoshitomo Sakuma, Keiko Sameshima, and Ryuji Kohno, "An Evaluation Considering Extention Of Surgery In The Adaptive Scheme Of Controlling Dosage By Model Predictive Controll," 2016 IEICE Society Conference, no.B-20-20, Sept. 2016. (in Japanese)

(2) Yoshitomo Sakuma, Kento Takabayashi, Chika Sugimoto, and Ryuji Kohno, "A Study about Control Scheme of Anesthesia Based on Prediction Model with Recurrent Neural Network," 2018 IEICE Society Conference, no. B-20-8, Sept. 2018. (in Japanese)

(3) Yoshitomo Sakuma, Chika Sugimoto, and Ryuji Kohno, "A Study about Prediction of Hypnotic and Analgesic Effect during Surgery with Recurrent Neural Network," 2019 IEICE General Conference, no. B-20-5, March 2019. (in Japanese)

Bibliography

[1] Health Quality Ontario et al. "Bispectral index monitor: an evidence-based analysis". *Ont Health Technol Assess Ser*, 4(9):1–70, 2004.

[2] C. M. Ionescu, R. De Keyser, and M. M. R. F. Struys. "Evaluation of a propofol and remifentanil interaction model for predictive control of anesthesia induction". In *2011 50th IEEE Conference on Decision and Control and European Control Conference*, pages 7374–7379, 2011.

[3] E. Furutani, K. Tsuruoka, S. Kusudo, G. Shirakami, and K. Fukuda. "a hypnosis and analgesia control system using a model predictive controller in total intravenous anesthesia during day-case surgery". In *Proceedings of SICE Annual Conference 2010*, pages 223–226, 2010.

[4] R. Mothkur and K. M. Poornima. "Machine learning will transfigure medical sector: A survey". In *2018 International Conference on Current Trends towards Converging Technologies (ICCTCT)*, pages 1–8, March 2018.

[5] Kenji SUZUKI. "Survey of deep learning applications to medical image analysis". *Medical Imaging Technology*, 35(4):212–226, 2017.

[6] Pratik Shah, Francis Kendall, Sean Khozin, Ryan Goosen, Jianying Hu, Jason Laramie, Michael Ringel, and Nicholas Schork. "Artificial intelligence and machine learning in clinical development: a translational perspective". *NPJ digital medicine*, 2(1):1–5, 2019.

[7] Junzo Takeda. "Measures to address the manpower shortage in anesthesiology in japan". *JAPAN MEDICAL ASSOCIATION JOURNAL*, 50(4):325, 2007.

[8] Ronald D Miller and William L Lanier. "The shortage of anesthesiologists: an unwelcome lesson for other medical specialties". In *Mayo Clinic Proceedings*, volume 76, pages 969–970. Elsevier, 2001.

[9] R Alexander and NG Volpe. "Total intravenous anesthesia". In *Anaesthesia, Pain, Intensive Care and Emergency Medicine—APICE*, pages 819–823. Springer, 2002.

[10] L. A. Paz, M. M. Silva, S. Esteves, R. Rabico, and T. Mendonca. "Automated total intravenous anesthesia (amtiva) from induction to recovery". In *2014 IEEE International Symposium on Medical Measurements and Applications (MeMeA)*, pages 1–6, June 2014.

[11] S. Zavitsanou, A. Mantalaris, M. C. Georgiadis, and E. N. Pistikopoulos. "In silico closed-loop control validation studies for optimal insulin delivery in type 1 diabetes". *IEEE Transactions on Biomedical Engineering*, 62(10):2369–2378, 2015.

[12] Y. Wang, H. Xie, X. Jiang, and B. Liu. "Intelligent closed-loop insulin delivery systems for icu patients". *IEEE Journal of Biomedical and Health Informatics*, 18(1):290–299, 2014.

[13] Y. Sakuma, K. Sameshima, and R. Kohno. "An adaptive scheme of controlling dosage and dosing interval in general anesthesia by model predictive control using anesthetic depth model". In *2017 11th International Symposium on Medical Information and Communication Technology (ISMICT)*, pages 77–81, Feb 2017.

[14] I. Nascu, A. Krieger, C. M. Ionescu, and E. N. Pistikopoulos. "Advanced model-based control studies for the induction and maintenance of intravenous anaesthesia". *IEEE Transactions on Biomedical Engineering*, 62(3):832–841, March 2015.

[15] Adriana Savoca, Jessica Barazzetta, Giuseppe Pesenti, and Davide Manca. "Model predictive control for automated anesthesia". In Anton Friedl, Jiří J. Klemeš, Stefan Radl, Petar S. Varbanov, and Thomas Wallek, editors, *28th European Symposium on Computer Aided Process Engineering*, volume 43 of *Computer Aided Chemical Engineering*, pages 1631 – 1636. Elsevier, 2018.

[16] Alexandra Krieger and Efstratios N. Pistikopoulos. "Model predictive control of anesthesia under uncertainty". *Computers & Chemical Engineering*, 71:699 – 707, 2014.

[17] Deepak D. Ingole, D. N. Sonawane, Vihangkumar V. Naik, Divyesh L. Ginoya, and Vedika Patki. "Implementation of model predictive control for closed loop control of anesthesia". In Vinu V. Das and Yogesh Chaba, editors, *Mobile Communication and Power Engineering*, pages 242–248, Berlin, Heidelberg, 2013. Springer Berlin Heidelberg.

[18] Ioana Nascu and Efstratios N. Pistikopoulos. "A multiparametric model-based optimization and control approach to anaesthesia". *The Canadian Journal of Chemical Engineering*, 94(11):2125–2137, 2016.

[19] Dr med Schnider, Thomas W., MB ChB Minto, Charles F., MD Gambus, Pedro L., MD Andresen, Corina, DDS PhD Goodale, David B., MD Shafer, Steven L., and MD Youngs, Elizabeth J. "The influence of method of administration and covariates on the pharmacokinetics of propofol in adult volunteers". *Anesthesiology: The Journal of the American Society of Anesthesiologists*, 88(5):1170–1182, 05 1998.

[20] Y. Sawaguchi, E. Furutani, G. Shirakami, M. Araki, and K. Fukuda. "A model-predictive hypnosis control system under total intravenous anesthesia". *IEEE Transactions on Biomedical Engineering*, 55(3):874–887, March 2008.

[21] Saba Rezvanian, Farzad Towhidkhah, Nematollah Ghahramani, and Alireza Rezvanian. "Increasing robustness of the anesthesia process from difference patient's delay using a state-space model predictive controller". *Procedia Engineering*, 15:928 – 932, 2011. CEIS 2011.

[22] S. Rezvanian, F. Towhidkhah, and N. Ghahramani. "Controlling the depth of anesthesia using model predictive controller and extended kalman filter". In *2011 1st Middle East Conference on Biomedical Engineering*, pages 213–216, Feb 2011.

[23] Rakesh Vaja, Larry McNicol, and Imogen Sisley. "Anaesthesia for patients with liver disease". *Continuing Education in Anaesthesia Critical Care & Pain*, 10(1):15–19, 12 2009.

[24] Jaouher Ben Ali, Takoua Hamdi, Nader Fnaiech, Véronique Di Costanzo, Farhat Fnaiech, and Jean-Marc Ginoux. "Continuous blood glucose level prediction of type 1 diabetes based on artificial neural network". *Biocybernetics and Biomedical Engineering*, 38(4):828 – 840, 2018.

[25] Fayrouz Allam, Zaki Nossai, Hesham Gomma, Ibrahim Ibrahim, and Mona Abdelsalam. "A recurrent neural network approach for predicting glucose concentration in type-1 diabetic patients". In Lazaros Iliadis and Chrisina Jayne, editors, *Engineering Applications of Neural Networks*, pages 254–259, Berlin, Heidelberg, 2011. Springer Berlin Heidelberg.

[26] Hyung-Chul Lee, Ho-Geol Ryu, Eun-Jin Chung, and Chul-Woo Jung. "Prediction of bispectral index during target-controlled infusion of propofol and remifentanil: A deep learning approach". *Anesthesiology: The Journal of the American Society of Anesthesiologists*, 128(3):492–501, 03 2018.

[27] A. M. LYAPUNOV. "The general problem of the stability of motion". *International Journal of Control*, 55(3):531–534, 1992.

[28] Zhong-Ping Jiang and Yuan Wang. "Input-to-state stability for discrete-time nonlinear systems". *Automatica*, 37(6):857 – 869, 2001.

[29] Léon Bottou. "Online learning and stochastic approximations". *On-line learning in neural networks*, 17(9):142, 1998.

[30] Andrii Shalaginov and Katrin Franke. "Big data analytics by automated generation of fuzzy rules for network forensics readiness". *Applied Soft Computing*, 52:359 – 375, 2017.

[31] Sebastian Ruder. "An overview of gradient descent optimization algorithms", 2017.

[32] Diederik P. Kingma and Jimmy Ba. "Adam: A method for stochastic optimization", 2017.

[33] GR Park. "Sedation, analgesia and muscle relaxation and the critically ill patient". *Canadian journal of anaesthesia*, 44(1):R40–R51, 1997.

[34] R.P.F. Scott, D.A. Saunders, and J. Norman. "Propofol: clinical strategies for preventing the pain of injection". *Anaesthesia*, 43(6):492–494, 1988.

[35] Miklos D Kertai, Elizabeth L Whitlock, and Michael S Avidan. "Brain monitoring with electroencephalography and the electroencephalogram-derived bispectral index during cardiac surgery". *Anesthesia and analgesia*, 114(3):533, 2012.

[36] Chanannait Paisansathan, Mukadder D Ozcan, Qaiser S Khan, Verna L Baughman, and Mehmet S Ozcan. "Signal persistence of bispectral index and state entropy during surgical procedure under sedation". *The Scientific World Journal*, 2012, 2012.

[37] J. G. Ziegler and N. B. Nichols. "Optimum settings for automatic controllers". *Journal of Dynamic Systems, Measurement, and Control*, 115(2B):220–222, 06 1993.